

In situ dehydration behavior of zeolite-like cavansite: A single-crystal X-ray study

ROSA MICAELA DANISI,* THOMAS ARMBRUSTER, AND BILJANA LAZIC

Mineralogical Crystallography, Institute of Geological Sciences, University of Bern, Freiestrasse 3, CH-3012 Bern, Switzerland

ABSTRACT

To track dehydration behavior of cavansite, $\text{Ca}(\text{VO})(\text{Si}_4\text{O}_{10}) \cdot 4\text{H}_2\text{O}$ [space group $Pnma$, $a = 9.6329(2)$, $b = 13.6606(2)$, $c = 9.7949(2)$ Å, $V = 1288.92(4)$ Å³] single-crystal X-ray diffraction data on a crystal from Wagholi quarry, Poona district (India) were collected up to 400 °C in steps of 25 °C up to 250 °C and in steps of 50 °C between 250 and 400 °C. The structure of cavansite is characterized by layers of silicate tetrahedra connected by V^{4+}O_5 square pyramids. This way a porous framework structure is formed with Ca and H₂O as extraframework occupants. At room temperature, the hydrogen bond system was analyzed. Ca is eightfold coordinated by four bonds to O of the framework structure and four bonds to H₂O molecules. H₂O linked to Ca is hydrogen bonded to the framework and also to adjacent H₂O molecules. The dehydration in cavansite proceeds in four steps.

At 75 °C, H₂O at O9 was completely expelled leading to 3 H₂O pfu with only minor impact on framework distortion and contraction [$V = 1282.73(3)$ Å³]. The Ca coordination declined from originally eightfold to sevenfold and H₂O at O7 displayed positional disorder.

At 175 °C, the split O7 sites approached the former O9 position. In addition, the sum of the three split positions O7, O7a, and O7b decreased to 50% occupancy yielding 2 H₂O pfu accompanied by a strong decrease in volume [$V = 1206.89(8)$ Å³]. The Ca coordination was further reduced from sevenfold to sixfold.

At 350 °C, H₂O at O8 was released leading to a formula with 1 H₂O pfu causing additional structural contraction ($V = 1156(11)$ Å³). At this temperature, Ca adopted fivefold coordination and O7 rearranged to disordered positions closer to the original O9 H₂O site.

At 400 °C, cavansite lost crystallinity but the VO²⁺ characteristic blue color was preserved. Stepwise removal of water is discussed on the basis of literature data reporting differential thermal analyses, differential thermo-gravimetry experiments and temperature dependent IR spectra in the range of OH stretching vibrations.

Keywords: Cavansite, dehydration, crystal structure, hydrogen bonding

INTRODUCTION

Cavansite, $\text{Ca}(\text{VO})(\text{Si}_4\text{O}_{10}) \cdot 4\text{H}_2\text{O}$, is a porous layer silicate, dimorphous with pentagonite. The mineral's name is derived from the chemical elements of which it is composed: calcium (ca-), vanadium (-van-), and silicon (-si). Discovered in 1960 at Owyhee Dam, Malheur County (Oregon, U.S.A.), cavansite is a relatively rare mineral (Staples et al. 1973). It occurs in cavities and veinlets in basalt and vugs in tuff as radiating greenish-blue prismatic crystals associated with calcite, analcime, thomsonite, heulandite, stilbite, and apophyllite (Staples et al. 1973). However, the largest and best samples come from Poona district in India where cavansite occurs in tholeiitic basalts of the Deccan Volcanic Province (Phadke and Apte 1994), and in pores of altered basalt breccias and tuffaceous andesite in association with calcite, heulandite, stilbite, and rare apophyllite (Powar and Byrappa 2001). More recently, cavansite has also been reported from basalts in Rio Grande do Sul in southern Brazil (Frank et al. 2005) and from Aranga quarry, Kaipara district, North Island New Zealand (Thornton 2004).

The structure of cavansite was solved by Evans (1973)

but crystal quality and experimental setup did not allow the determination of hydrogen positions. However, Solov'ev et al. (1993) reported the location of the hydrogen atoms attached to H₂O molecules. Corresponding identifications of hydrogen-bond systems have recently been repeated by Hughes et al. (2011).

The atomic arrangement in cavansite consists of undulating pyroxenoid-like $(\text{SiO}_3)_n$ chains joined laterally into sheets parallel to the **a**-c plane to form a network of four-and eight-membered rings in (010). Adjacent chains have the tetrahedral apices pointing alternately up and down along the **b** axes (Evans 1973). The sheets are cross-linked via the basal square of VO₅ pyramids, which are completed by one short apical V-O bond of ca. 1.6 Å (e.g., Evans 1973; Solov'ev et al. 1993; Hughes et al. 2011) named vanadyl group. This VO²⁺ ion is responsible for the brilliant sky blue color of the crystals (Rossman 2011). A porous three-dimensional framework is formed by the linkage of tetrahedral sheets with VO₅ square pyramids. Large cavities in the structure are occupied in zeolite-like fashion by Ca and coordinating H₂O molecules. Calcium has four bonds to oxygen atoms of silicate tetrahedra and four bonds to H₂O molecules completing an eightfold coordination.

The cavansite framework shows strong similarities to that of gismondine, $\text{CaAl}_2\text{Si}_2\text{O}_8 \cdot 4\text{H}_2\text{O}$. However, in gismondine the exposed

* E-mail: rosa.danisi@krist.unibe.ch

tetrahedral apices in adjacent layers are linked directly to each other to form a three-dimensional aluminosilicate network (Fischer 1963) and not via vanadyl-type VO_5 square pyramids as in cavansite.

The dimorphism of cavansite and pentagonite is based on the difference in linkages in the silicate layer. Undulating $(\text{SiO}_3)_n$ chains are discernible in both, but in cavansite these chains are joined laterally into sheets made up of fourfold and eightfold rings, while in pentagonite they are differently joined so that only sixfold rings are formed (Evans 1973).

Cavansite has not yet been synthesized in the laboratory but other open-framework silicates containing vanadium are reported. Wang et al. (2002) describe two open-framework vanadosilicates, VSH-1K and VSH-2Cs that contain a similar structural motif found in the natural minerals cavansite and pentagonite. Moreover, a series of novel vanadium silicates with open-framework and microporous structures has been synthesized under mild hydrothermal conditions with free channel diameters as large as 6.5 Å (Wang et al. 2002). Ten distinct framework types containing vanadyl groups have been identified and show a great potential to be used as molecular sieves or in catalysis due to their high thermal stability and ion-exchange properties (Wang et al. 2002).

Previous structural studies of the dehydration behavior of cavansite are limited to a room-temperature single-crystal X-ray diffraction experiment of a crystal previously partly dehydrated under vacuum at 220 °C (Rinaldi et al. 1975). In addition, differential thermal analysis (DTA) and differential thermo-gravimetry (DTG) (Phadke and Apte 1994; Powar and Byrappa 2001; Ishida

et al. 2009), in situ FTIR and Raman spectroscopy (Prasad and Prasad 2007) were done.

The aim of this study is to further characterize the hydrogen-bond system and the in situ dehydration behavior of cavansite using single-crystal X-ray diffraction on crystals from Wagholi quarry, Poona district (India). This investigation was initiated by a supposed contradiction: Solov'ev et al. (1993) report H_2O III with the highest atomic displacement parameter and the longest bond to Ca, also confirmed by Hughes et al. (2011). At first glance, one should assume that, upon heating, H_2O III with the weakest bond is expelled first. However, the structural study of partly dehydrated cavansite by Rinaldi et al. (1975) indicates that H_2O (their W1) close to H_2O III (room temperature) is the most stable one before complete dehydration occurs accompanied with structural breakdown.

EXPERIMENTAL METHODS

A cavansite single crystal from Wagholi, Poona district, Maharashtra, India of approximate dimensions $0.1 \times 0.1 \times 0.5$ mm was selected for our structure study and mounted in an open 0.1 mm diameter quartz-glass capillary.

Single-crystal X-ray diffraction data were collected with a Bruker APEX II diffractometer using $\text{MoK}\alpha$ ($\lambda = 0.71073$ Å) X-ray radiation with 50 kV and 30 mA X-ray power. To study in situ dehydration, complete data sets were collected in steps of 25 °C up to 250 °C and in steps of 50 °C up to 400 °C using a self-constructed temperature controlled hot nitrogen blower. Before data collections the crystal was kept at least 30 min at the next measuring temperature.

CCD area-detector data were integrated and an empirical absorption correction was applied using the Apex2 v. 2011.4-1 software package. Data-collection parameters and refinement parameters are given in Table 1. Neutral atom scattering-factors were used for structure refinement with SHELXL-97 (Sheldrick 2008). Hydrogen positions were extracted from difference-Fourier maps applying the restraint H-O

TABLE 1. Parameters for X-ray data collection and crystal-structure refinement of cavansite

	Cavansite (RT)	Cavansite (75 °C)	Cavansite (175 °C)	Cavansite (350 °C)
Crystal data				
Unit-cell dimensions (Å)	$a = 9.6329(2)$ $b = 13.6606(2)$ $c = 9.7949(2)$ 1288.92(4) $Pnma$ (No. 62) 4 $\text{Ca}(\text{VO})(\text{Si}_4\text{O}_{10}) \cdot 4\text{H}_2\text{O}$	$a = 9.6090(10)$ $b = 13.6833(2)$ $c = 9.7559(2)$ 1282.73(3) $Pnma$ (No. 62) 4 $\text{Ca}(\text{VO})(\text{Si}_4\text{O}_{10}) \cdot 3\text{H}_2\text{O}$	$a = 9.4746(4)$ $b = 13.2620(5)$ $c = 9.6050(4)$ 1206.89(8) $Pnma$ (No. 62) 4 $\text{Ca}(\text{VO})(\text{Si}_4\text{O}_{10}) \cdot 2\text{H}_2\text{O}$	$a = 9.39(5)$ $b = 13.11(8)$ $c = 9.39(5)$ 1156(11) $Pnma$ (No. 62) 4 $\text{Ca}(\text{VO})(\text{Si}_4\text{O}_{10}) \cdot 1\text{H}_2\text{O}$
Volume (Å ³)	1288.92(4)	1282.73(3)	1206.89(8)	1156(11)
Space group	$Pnma$ (No. 62)	$Pnma$ (No. 62)	$Pnma$ (No. 62)	$Pnma$ (No. 62)
Z	4	4	4	4
Chemical formula	$\text{Ca}(\text{VO})(\text{Si}_4\text{O}_{10}) \cdot 4\text{H}_2\text{O}$	$\text{Ca}(\text{VO})(\text{Si}_4\text{O}_{10}) \cdot 3\text{H}_2\text{O}$	$\text{Ca}(\text{VO})(\text{Si}_4\text{O}_{10}) \cdot 2\text{H}_2\text{O}$	$\text{Ca}(\text{VO})(\text{Si}_4\text{O}_{10}) \cdot 1\text{H}_2\text{O}$
Intensity measurement				
Crystal shape	prismatic	prismatic	prismatic	prismatic
Crystal size (mm)	$0.1 \times 0.1 \times 0.5$	$0.1 \times 0.1 \times 0.5$	$0.1 \times 0.1 \times 0.5$	$0.1 \times 0.1 \times 0.5$
Diffractometer	APEX II SMART	APEX II SMART	APEX II SMART	APEX II SMART
X-ray radiation	$\text{MoK}\alpha \lambda = 0.71073$ Å	$\text{MoK}\alpha \lambda = 0.71073$ Å	$\text{MoK}\alpha \lambda = 0.71073$ Å	$\text{MoK}\alpha \lambda = 0.71073$ Å
X-ray power	50 kV, 30 mA	50 kV, 30 mA	50 kV, 30 mA	50 kV, 30 mA
Monochromator	graphite	graphite	graphite	graphite
Temperature	293 K	348 K	448 K	623 K
Time per frame	10 s	10 s	10 s	10 s
Max. θ	30.5	30.5	30.5	30.5
Index ranges	$-13 \leq h \leq 13$ $-19 \leq k \leq 19$ $-13 \leq l \leq 13$	$-13 \leq h \leq 13$ $-19 \leq k \leq 19$ $-13 \leq l \leq 13$	$-12 \leq h \leq 13$ $-18 \leq k \leq 18$ $-7 \leq l \leq 13$	$-10 \leq h \leq 10$ $-14 \leq k \leq 14$ $-10 \leq l \leq 10$
No. of measured reflections	10723	16172	7406	4845
No. of unique reflections	2039	2027	1900	916
No. of observed reflections [$l > 2\sigma(l)$]	1859	1864	1644	731
Refinement of the structure				
No. of parameters used in refinement	116 + 7 restraints	105	102	102
R_{int}	0.0258	0.0280	0.0328	0.0531
R_{σ}	0.0188	0.0154	0.0292	0.0382
$R1, l > 2\sigma(l)$	0.0232	0.0294	0.0295	0.0593
$R1, \text{all data}$	0.0262	0.0323	0.0369	0.0783
wR2 (on F^2)	0.0682	0.0856	0.0901	0.1833
GooF	1.057	1.068	0.988	1.149
Δp_{\min} (-e/Å ³)	-0.58 close to V	-0.73 close to O7b	-0.56 close to V	-0.78 close to V
Δp_{\max} (e/Å ³)	0.49 close to O3	0.87 close to O8	0.74 close to O7	0.79 close to Ca

$= 0.95(1)$ Å and refined with fixed isotropic displacement parameters. The experimentally derived hydrogen-bond system was confirmed by using bond-valence calculations (Brown and Altermatt 1985).

Initial atomic labels were those of Evans (1973) but the standard space-group setting *Pnma* was chosen in contrast to *Pcmm* preferred by Evans (1973) requiring interchange of *a* and *c*. The final refinement for the data collected at room temperature, based on 1859 observed reflections and 116 parameters with 7 restraints, converged at $R_1 = 0.0232$. Refinements for the data collected at 75, 175, and 350 °C converged at $R_1 = 0.0294$, $R_1 = 0.0295$, and $R_1 = 0.0593$, respectively. The smaller data sets reported at 175 °C and 350 °C (Table 1) are due to experimental problems. Between 150 and 175 °C, the crystal broke and only a limited number of reflections could be integrated. For 175 and 350 °C data, O positions of partly occupied H₂O sites were refined with common isotropic displacement parameters constrained to each other.

RESULTS AND DISCUSSION

Atomic coordinates and displacement parameters for the cavansite structure at room temperature, 75, 175, and 350 °C are given in Tables 2 and 3¹, respectively. Selected distances and angles of hydrogen bonds under ambient conditions are in Table 4. Table 5¹ compares the interatomic distances at room temperature, 75, 175, and 350 °C. Results of bond valence calculations for cavansite at room temperature are reported in Table 6¹. (CIFs¹ are also available.)

Our structural study under ambient conditions confirmed the framework structure built by tetrahedral layers connected by vanadyl-type VO₅ square-based pyramids (Figs. 1–3) as reported

by Evans (1973), Rinaldi et al. (1975), Solov'ev et al. (1993), and Hughes et al. (2011).

Moreover, we located the H atoms and defined the hydrogen-bond system (Figs. 1a–b and 3a). Our structure refinement with five located H positions indicates that there are three hydrogen bonds with H–O acceptor distances between 2.08 and 2.17 Å: O9–H9a–O6, O7–H7a–O9, and O7–H7b–O5. H8 is fixed by only weak hydrogen bonds and the corresponding H–O acceptor distance for the O8–H8–O3 hydrogen bond is 2.64 Å with d(O8–O3) = 3.56 Å. In general, the hydrogen bond system defined by us is similar to the findings by Solov'ev et al. (1993) and Hughes et al. (2011). The O6–H9a interaction links the CaO₄(H₂O)₄ polyhedron to the opposing apex of the V square-based pyramid (Fig. 1a), while the O5–H7b and O3–H8 interactions link the silicate layer to the extraframework occupants (Fig. 3a). The O9–H7a interaction, not reported in the study of Solov'ev et al. (1993) and Hughes et al. (2011), connects two H₂O molecules located inside the elliptical channels parallel to **b** formed by eight-membered rings of tetrahedra. Solov'ev et al. (1993) and Ishida et al. (2009) assumed other interactions (Table 7). In particular, the angle between donor-hydrogen-acceptor (DHA) is probably too narrow (less than 120°) for the assumed hydrogen bonds (H₂O)1–H2–O4, (H₂O)2–H3–O3 and (H₂O)3–H5–O6 (Solov'ev et al. 1993).

TABLE 2a. Atomic coordinates and U_{eq} (U_{iso}) (Å²) values for cavansite at RT

Site	Occ.	x	y	z	U_{eq}
V	1	0.02594(4)	0.25	0.09618(4)	0.01042(9)
Ca	1	-0.38231(4)	0.75	-0.08263(5)	0.01275(10)
Si1	1	-0.18305(4)	0.53318(3)	-0.09496(4)	0.00808(9)
Si2	1	-0.10728(4)	0.45691(3)	0.18382(4)	0.00766(9)
O1	1	-0.17796(11)	0.65027(8)	-0.08597(11)	0.0128(2)
O2	1	-0.08731(12)	0.34231(8)	0.20600(11)	0.0137(2)
O3	1	-0.20339(11)	0.47968(9)	0.05164(11)	0.0144(2)
O4	1	-0.04191(11)	0.48914(8)	-0.16578(11)	0.0122(2)
O5	1	-0.31477(11)	0.49541(8)	-0.18514(11)	0.0112(2)
O6	1	-0.0430(2)	0.25	-0.05191(19)	0.0237(4)
O7	1	-0.46993(18)	0.88139(14)	0.05339(19)	0.0442(4)
H7a	1	-0.421(3)	0.869(3)	0.136(2)	0.080*
H7b	1	-0.5615(16)	0.891(3)	0.081(4)	0.080*
O8	1	-0.6383(2)	0.75	-0.1258(3)	0.0374(5)
H8	1	-0.685(3)	0.6944(17)	-0.093(3)	0.080*
O9	1	-0.2832(4)	0.75	0.1898(4)	0.0775(11)
H9a	1	-0.330(5)	0.75	0.276(3)	0.080*
H9b	1	-0.192(2)	0.75	0.230(5)	0.080*

* U_{iso} of hydrogen was fixed.

TABLE 2b. Atomic coordinates and U_{eq} (U_{iso}) (Å²) values for cavansite at 75 °C

Site	Occ.	x	y	z	U_{eq}
V	1	0.02600(5)	0.25	0.09027(4)	0.01219(11)
Ca	1	-0.38248(5)	0.75	-0.08753(5)	0.01422(12)
Si1	1	-0.18529(5)	0.53429(4)	-0.09246(5)	0.00969(11)
Si2	1	-0.10434(5)	0.45653(3)	0.18578(5)	0.00934(12)
O1	1	-0.17964(14)	0.65118(10)	-0.08307(14)	0.0150(3)
O2	1	-0.08347(15)	0.34199(10)	0.20472(14)	0.0169(3)
O3	1	-0.20289(14)	0.48168(11)	0.05573(14)	0.0174(3)
O4	1	-0.04573(13)	0.49007(10)	-0.16576(14)	0.0146(3)
O5	1	-0.31993(13)	0.49792(10)	-0.17994(13)	0.0138(3)
O6	1	-0.0455(3)	0.25	-0.0566(2)	0.0294(5)
O7	0.270(8)	-0.4471(11)	0.8517(9)	0.1035(13)	0.0448(11)*
O7a	0.245(7)	-0.3993(11)	0.8184(8)	0.1464(11)	0.0448(11)*
O7b	0.557(10)	-0.4643(5)	0.8806(4)	0.0570(6)	0.0448(11)*
O8	1	-0.6396(4)	0.75	-0.0987(5)	0.0756(14)
O9	0.105(8)	-0.295(3)	0.75	0.188(3)	0.0448(11)*

* U_{iso} of oxygen was constrained to a common isotropic displacement parameter.

¹ Deposit item AM-12-079, Tables 3, 5, and 6, and CIFs. Deposit items are available two ways: For a paper copy contact the Business Office of the Mineralogical Society of America (see inside front cover of recent issue) for price information. For an electronic copy visit the MSA web site at <http://www.minsocam.org>, go to the *American Mineralogist* Contents, find the table of contents for the specific volume/issue wanted, and then click on the deposit link there.

TABLE 2c. Atomic coordinates and U_{eq} (U_{iso}) (Å²) values for cavansite at 175 °C

Site	Occ.	x	y	z	U_{eq}
V	1	0.03479(5)	0.25	0.09988(5)	0.01642(12)
Ca	1	-0.38889(6)	0.75	-0.07578(6)	0.01849(14)
Si1	1	-0.19261(6)	0.52653(4)	-0.08317(6)	0.01415(13)
Si2	1	-0.09206(6)	0.46155(4)	0.19910(6)	0.01366(13)
O1	1	-0.18823(15)	0.64770(11)	-0.07596(16)	0.01993(3)
O2	1	-0.05978(17)	0.34527(11)	0.22691(16)	0.0218(3)
O3	1	-0.20100(16)	0.47554(13)	0.07010(16)	0.0226(3)
O4	1	-0.05458(16)	0.48034(11)	-0.16282(16)	0.0196(3)
O5	1	-0.33434(16)	0.48941(11)	-0.16389(15)	0.0189(3)
O6	1	-0.0552(3)	0.25	-0.0398(3)	0.0337(6)
O7	0.162(12)	-0.430(2)	0.7778(16)	0.1679(16)	0.044(3)*
O7a	0.203(10)	-0.3625(16)	0.7750(11)	0.1759(12)	0.044(3)*
O7b	0.142(14)	-0.397(3)	0.810(2)	0.161(2)	0.044(3)*
O8	1	-0.6409(5)	0.75	-0.0485(8)	0.121(2)

* U_{iso} of oxygen was constrained to a common isotropic displacement parameter.

TABLE 2d. Atomic coordinates and U_{eq} (U_{iso}) (Å²) values for cavansite at 350 °C

Site	Occ.	x	y	z	U_{eq}
V	1	0.0374(2)	0.25	0.0993(2)	0.0323(6)
Ca	1	-0.3884(3)	0.75	-0.0715(3)	0.0373(8)
Si1	1	-0.1968(2)	0.52399(16)	-0.0781(2)	0.0256(6)
Si2	1	-0.0833(2)	0.46265(16)	0.2073(2)	0.0243(6)
O1	1	-0.1921(6)	0.6461(4)	-0.0706(7)	0.0373(15)
O2	1	-0.0485(6)	0.3461(4)	0.2374(6)	0.0378(15)
O3	1	-0.1946(6)	0.4739(5)	0.0777(6)	0.0366(15)
O4	1	-0.0631(5)	0.4784(4)	-0.1666(6)	0.0309(14)
O5	1	-0.3434(6)	0.4873(4)	-0.1524(6)	0.0310(14)
O6	1	-0.0568(12)	0.25	-0.0373(12)	0.0613(3)
O7	0.25(3)	-0.517(6)	0.780(4)	0.134(6)	0.129(18)*
O7b	0.22(3)	-0.415(7)	0.782(4)	0.181(6)	0.129(18)*
O8	0.24(4)	-0.590(9)	0.75	0.018(10)	0.129(18)*

* U_{iso} of oxygen was constrained to a common isotropic displacement parameter.

TABLE 4. Hydrogen bond distances (\AA) and O-H \cdots O angles ($^{\circ}$)

Species	D-H	H \cdots A	D \cdots A	\angle (DHA)	Hydrogen bond
H_2O	0.957(10)	2.081(12)	3.033(4)	173(5)	O9-H9a \cdots O6
H_2O	0.946(10)	2.17(3)	2.871(4)	130(3)	O7-H7a \cdots O9
H_2O	0.939(10)	2.642(13)	3.564(2)	167(3)	O8-H8 \cdots O3
H_2O	0.934(10)	2.12(3)	2.897(2)	140(3)	O7-H7b \cdots O5

Notes: Hydrogen positions were determined with the restraint O-H is 0.95(2) \AA . D = donor; A = acceptor.

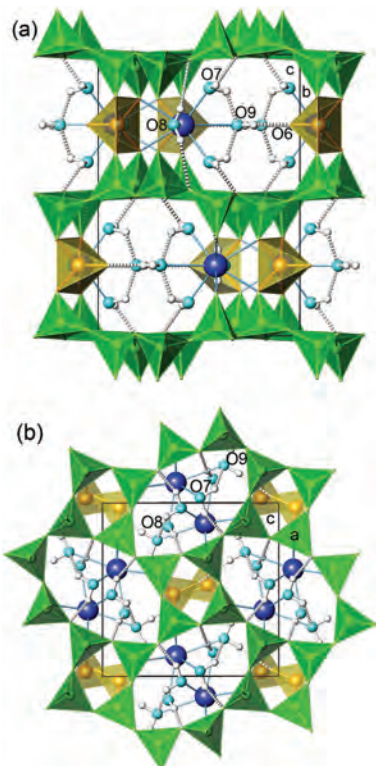


FIGURE 1. Framework of cavansite at room temperature. The green polyhedra represent Si tetrahedra, while the yellow polyhedra are the V square-based pyramids. Calcium is in blue and oxygen of H_2O are shown as light blue spheres with attached small white spheres representing H. Hydrogen-bond acceptor interactions are shown by gray dashed connectors. The water molecules O7, O8, and O9 are labeled. (a) Projection along the **a** axis showing the silica layers linked by vanadyl-type VO_5 square based pyramids. (b) View of the cavansite structure parallel to **b** showing the porous character of the structure high-lighting the four-and eight-member rings of tetrahedra. (Color online.)

TABLE 7. Hydrogen-bond system in Solov'ev et al. (1993), Ishida et al. (2009), Hughes et al. (2011), and the present study

Solov'ev et al. (1993)	Ishida et al. (2009)	Hughes et al. (2011)	This study
$(\text{H}_2\text{O})_1\text{-H}1\cdots\text{O}5$	O7-H1 \cdots O5	O7-H7b \cdots O5	O7-H7b \cdots O5
$(\text{H}_2\text{O})_1\text{-H}2\cdots\text{O}4$			O7-H7a \cdots O9
$(\text{H}_2\text{O})_2\text{-H}3\cdots\text{O}3$			O8-H8 \cdots O3
$(\text{H}_2\text{O})_3\text{-H}4\cdots\text{O}6$	O8-H2 \cdots O2		
$(\text{H}_2\text{O})_3\text{-H}5\cdots\text{O}6$	O8-H2 \cdots O1		
	O9-H3 \cdots O6	O9-H9a \cdots O6	O9-H9a \cdots O6
	O9-H4 \cdots O7		
	O9-H5 \cdots O7		

Moreover, Ishida et al. (2009) reported two hydrogen bonds (O9-H4 \cdots O7 and O9-H5 \cdots O7) with the distance between acceptor and hydrogen greater than 3.1 \AA and two hydrogen bonds (O8-H2 \cdots O2 and O8-H2 \cdots O1) with the DHA angle less than 120°. We did not consider the above interactions because they are not consistent with the geometric criterion for hydrogen bonds.

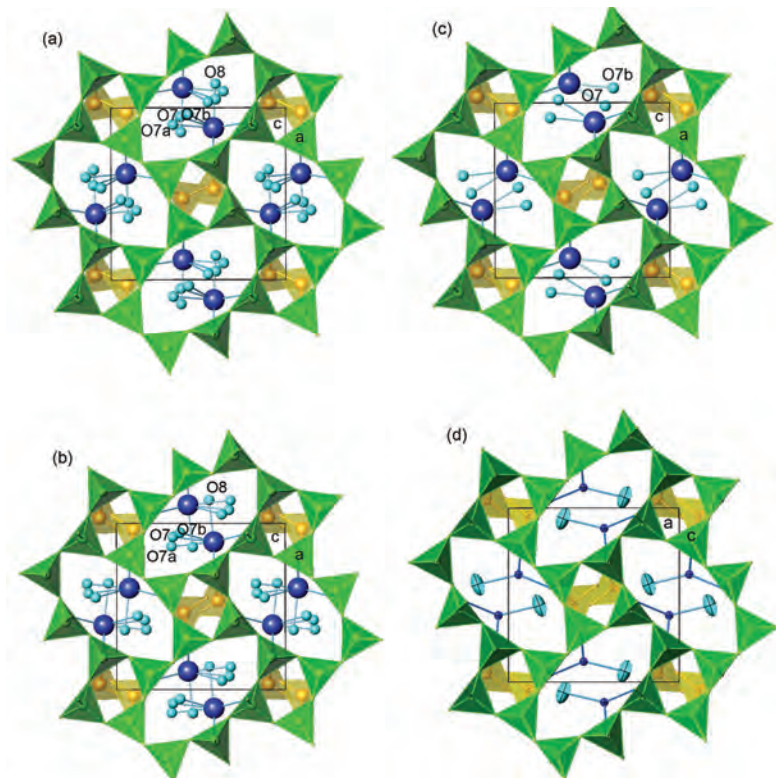
Without considering H in bond-valence calculations, the H_2O molecules are characterized by an oxygen bond-valence sum (bvs) < 0.5 valence units (v.u.). According to a model by Ferraris and Ivaldi (1988), which is here simplified, the bvs for a donor of a hydrogen bond may be increased by 0.8 v.u. and the bvs of acceptor oxygen may be increased by 0.2 v.u., indicating that O7, O8, and O9 represent H_2O molecules. This finding is in contrast to the interpretation of Ishida et al. (2009) suggesting, by applying the “valence-matching principle,” the existence of H_3O^+ and OH^- .

Our *in situ* dehydration experiments at elevated temperature and dry N_2 atmosphere showed that cavansite starts losing H_2O already at 50 °C. At this temperature, H_2O at O9 displayed positional disorder and was split into O9 and the subsite O9a, ca. 1 \AA apart. The sum of occupancies for O9 and O9a decreased to 0.84(4). Moreover, at 50 °C O7 was split into three positions (O7, O7a, and O7b) indicating substantial disorder. The distances between O7-O7a, O7-O7b, O7a-O7b, and O7b-O7b' are 0.45, 1.22, 0.79, and 2.28 \AA , respectively. The displacement onto three different positions probably models dynamic disorder.

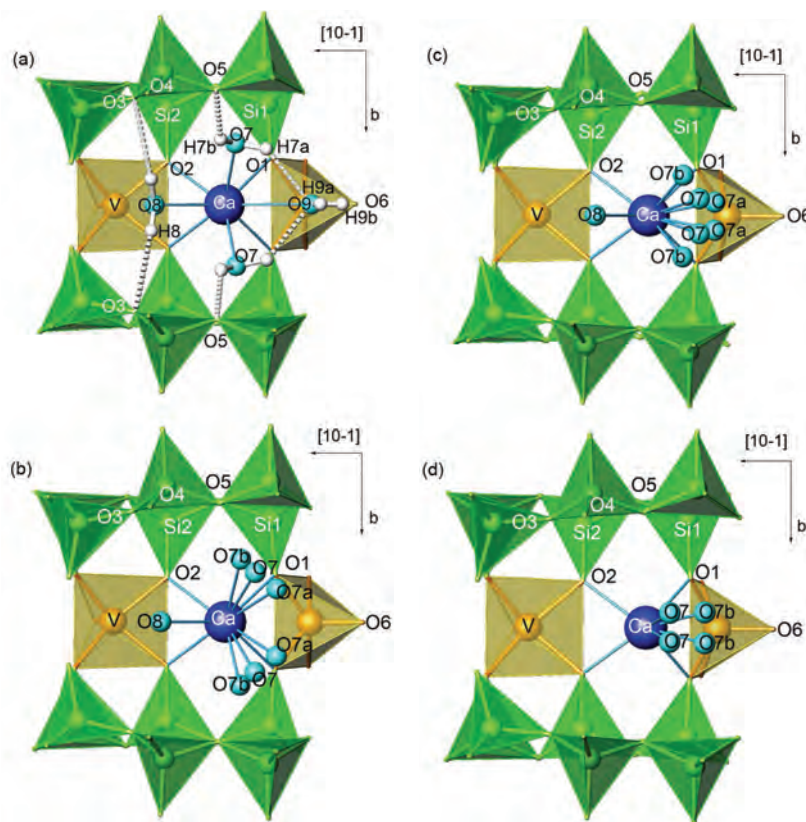
At 75 °C, the O9 site became almost vacant and the unit-cell volume decreased from 1288.92(4) \AA^3 at room temperature to 1282.73(3) \AA^3 leading to a formula with 3 H_2O pfu (Fig. 2a). The coordination of Ca decreased from eight to seven (Table 5¹) accompanied by shortening the mean Ca-O distance from 2.473 to 2.469 \AA .

At 175 °C, the displacement of O7 at three different positions was still observed but in a slightly modified arrangement (Fig. 2b). H_2O at the O7 subsites began to approach the former O9 position, on the mirror plane. In addition, the sum of the three displaced positions O7, O7a, and O7b decreased to 50% occupancy leading to a formula with 2 H_2O pfu. Decreased H_2O content reduced the volume to 1206.89(8) \AA^3 and Ca became sixfold coordinated with subsequent shortening of the mean Ca-O distance from 2.469 to 2.359 \AA . The release of H_2O molecules acts as a promoter of structural modification in the porous three-dimensional framework (Alberti and Martucci 2011). In particular, at 175 °C the angle between Si2-O5-Si1 decreased from 131.46(9)° to 128.24(10)° (Table 5¹) leading to a slight compression of the pore system due to the release of H_2O molecules.

From 200 to 350 °C the population of H_2O at O8 decreased from 1.0 to 0.24(4) while the displacement parameter at 350 °C became 3 times larger than at 200 °C due to assumed dynamic disorder. At 350 °C, O7 was split into two positions while the O7a site became empty. O7 and O7b together still preserved 50% occupation but moved closer to the original O9 H_2O site on the mirror plane. As a consequence of release of H_2O at O8 leading to a formula with 1 H_2O pfu (Fig. 2c), Ca adopted fivefold coordination associated with reduction of the unit-cell volume to 1156(11) \AA^3 . The release of H_2O at O8 led to a further decrease of the Si2-O5-Si1 angle to 126.2(4)° (Table 5¹) causing additional deformation of the pore system. Breakdown of the



◀ FIGURE 2. Framework of cavansite and channel occupants in space-group setting $Pnma$; (a) at 75 °C, (b) at 175 °C, and (c) at 350 °C. (d) Framework of cavansite by Rinaldi et al. (1975) showing only one H_2O molecule (W1) after dehydration at 220 °C under vacuum, refined at room temperature with anisotropic displacement parameters. The space group setting is $Pcmn$. (Color online.)



◀ FIGURE 3. Portion of the cavansite structure focusing on Ca coordination. (a) Cavansite at room temperature showing the hydrogen-bond system. The $O9-H9a\cdots O6$ hydrogen bond is not shown because it points toward the observer. (b) Cavansite at 75 °C. The H_2O molecule at $O9$ has been expelled and the H_2O molecule at $O7$ is split into three positions. The Ca coordination is reduced from eight to seven. (c) Cavansite at 175 °C. The sum of the three displaced positions $O7$, $O7a$, and $O7b$ was equal to 50% occupancy. The Ca coordination was reduced from sevenfold to sixfold. (d) Cavansite at 350 °C. The population at $O8$ is 0.24(4) and it is omitted in the picture. On average Ca is fivefold coordinated. (Color online.)

structure, observed at approximately 400 °C, probably resulted from removal of the residual H₂O molecule split at the O7 and O7b sites.

The crystal structure of partly dehydrated cavansite from Oregon, U.S.A., was reported by Rinaldi et al. (1975). After heating in vacuum at 220 °C only one water molecule per Ca was found in the structure (Fig. 2d). The results of Rinaldi et al. (1975) represent a dehydration state, which we observed in situ at 350 °C with the major difference that in their room-temperature data W1 was refined with anisotropic displacement parameters, whereas we used split positions (O7 and O7a) to model dynamic disorder at elevated temperature. Thus, due to the interaction of vacuum and heating the dehydration found by Rinaldi et al. (1975) occurred at lower temperature. The supposed contradiction that the H₂O molecule with the longest bond to Ca at room temperature (H₂O III of Solov'ev et al. 1993) is the most stable one upon dehydration (W1 of Rinaldi et al. 1975) could be explained. As expected, softly bonded H₂O III (O9 in this study) is released first (75 °C). However, with increasing temperature (above 175 °C) H₂O I of Solov'ev et al. 1993 (corresponding to O7 in this study) adopts a position close to the mirror plane, which roughly resembles the original O9 site. It is important to underline that the O7 subsites (this study; corresponding to W1 of Rinaldi et al. 1973) have much shorter distances to Ca (Table 5¹) than the original position of H₂O III (O9 in this study).

Our dehydration steps (Fig. 4) observed at different temperatures correlate with the thermo-gravimetric data reported by Phadke and Apte (1994), Powar and Byrappa (2001), Prasad and Prasad (2007), and Ishida et al. (2009) (Table 8). The four steps of weight loss in succession correspond to the expulsion of four water molecules, one at a time. The dehydration steps (from the DTA curves) at 95, 225, 350, and 450 °C (Ishida et al. 2009) are at higher temperatures than the transitions at 75, 175, 350, and 400 °C in our dehydration study. Moreover, above 500 °C (Prasad and Prasad 2007) and above 400 °C (this study) cavansite decomposes to an amorphous phase after losing the last H₂O molecule at O7. It should be considered that the temperature values reported for the DTA-DTG curves (Phadke and Apte 1994; Powar and Byrappa 2001; Prasad and Prasad 2007; Ishida et al. 2009) are referred to the peak and not to the onset of the steps of weight loss. This explains the different temperature values between the thermo-gravimetric data and our results.

The O-H stretching region in the wavelength range 4000 to 3000 cm⁻¹ of the IR spectrum of cavansite is characterized by four peaks at 3648, 3592, 3548, and 3490 cm⁻¹, and a shoulder at 3250 cm⁻¹ (Powar and Byrappa 2001). These results are in agreement with the spectra reported by Prasad and Prasad (2007) and Ishida et al. (2009). On the low-frequency tail of the OH-characteristic absorptions Ishida et al. (2009) reported an additional poorly

resolved absorption at 3186 cm⁻¹. Only the observed intense O-H modes at high wave numbers correlate with the observed donor-acceptor distances (Table 4). According to the hydrogen bond-length vs. IR frequency correlation by Libowitzky (1999) absorptions between 3490 and 3592 cm⁻¹ correspond to donor-acceptor (O-O) distances of ca. 2.9–3.5 Å, which agrees with the D-A distances in Table 4. The shoulders at 3250 and 3186 cm⁻¹ correspond to donor-acceptor distances of 2.72 Å and below. Such strong hydrogen bonds were not observed in terms of D-A distances for cavansite.

Prasad and Prasad (2007) also report an IR spectrum of the OH-characteristic region at 177 °C showing absorptions at 3561 and 3608 cm⁻¹ corresponding in intensity and shape to those at 3552 and 3606 cm⁻¹ found at room temperature. A trace of the 3250 cm⁻¹ absorption was still evident at 177 °C. Our structural study indicated that at 175 °C H₂O at O9 was expelled and O7 and subsites were half occupied. The room-temperature IR spectra (Powar and Byrappa 2001; Prasad and Prasad 2007; Ishida et al. 2009) may therefore be interpreted such that the band at 3648 cm⁻¹ is due to the very weak hydrogen bond O9-H9b-O? (not specified in our study) or to O9-H9a-O6. The band at 3490 cm⁻¹ is assigned to O7-H7-O9 in agreement (Table 4) with the hydrogen bond-length vs. IR frequency correlation by Libowitzky (1999).

Dehydration behavior as observed for cavansite is typical of zeolites and in particular of gismondine, CaAl₂Si₂O₈·4H₂O, which has a similar crystal structure (Rinaldi and Vezzalini

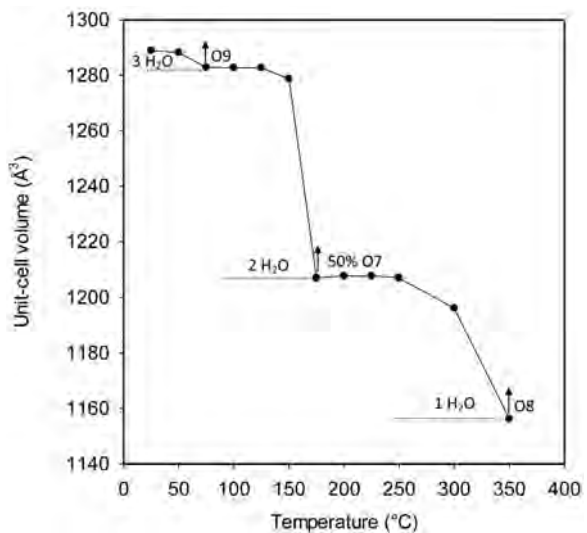


FIGURE 4. Development of unit-cell volume vs. temperature for in situ dehydration experiments of cavansite. With exception of the 350 °C data, the size of the symbols is larger than the associated e.s.d. values.

TABLE 8. Comparison between the results of thermo-gravimetric analysis of cavansite reported by Phadke and Apte (1994), Powar and Byrappa (2001), Prasad and Prasad (2007), and Ishida et al. (2009), all values in °C

Phadke and Apte (1994)	Powar and Byrappa (2001)	Prasad and Prasad (2007)	Ishida et al. (2009)
150	120 200	87 197	125
290		277	250
440			400
530		500	510

Note: Temperatures correspond to the maxima of DTG curves and not to the onset of dehydration.

1985; Vezzalini et al. 1993; Milazzo et al. 1998). As reported by Van Reeuwijk (1971), five metastable phases were created while heating gismondine, at ca. 70, 87, 108, 196, and 280 °C before final collapse. At 350 °C, a structural transformation takes place and the formation of high-temperature Ca-feldspar starts. Compared to cavansite, structural modifications in gismondine upon dehydration are much more severe. Between ambient conditions ($H_2O/Ca = 4$) and 160 °C ($H_2O/Ca = 2$) the normalized unit-cell volume of gismondine reduced by 17%, whereas in cavansite the volume change between room temperature ($H_2O/Ca = 4$) and 350 °C ($H_2O/Ca = 1$) amounts to only 10%. This difference is also corroborated by changes in T-O-T angles. In the temperature range cited above, average T-O-T angles in gismondine decrease from 146 to 132° (Rinaldi and Vezzalini 1985; Vezzalini et al. 1993) whereas average T-O-T angles in cavansite decrease from 132 to 130° (Table 5¹). Furthermore, in the course of dehydration gismondine undergoes several phase transitions (Milazzo et al. 1998), whereas in cavansite dehydration proceeds rather smoothly within the same space group. The limiting Ca coordination seems to be responsible for phase transitions or structural collapse in gismondine and cavansite before complete dehydration. The lowest Ca coordination number in cavansite appears to be five and removal of the last H_2O molecule caused structural destruction. The high-temperature structure of gismondine before structural breakdown has not been solved (Milazzo et al. 1998). Thus the limiting Ca coordination in gismondine remains unknown. The critical limit in Ca coordination has been reported for several Ca-containing zeolites but this limit alone cannot be taken as reference to determine the framework breakdown (Cruciani 2006).

ACKNOWLEDGMENTS

The constructive reviews of Giovanna Vezzalini and an anonymous referee are highly appreciated.

REFERENCES CITED

- Alberti, A. and Martucci, A. (2011) Reconstructive phase transitions in microporous materials: rules and factors affecting them. *Microporous and Mesoporous Materials*, 141, 192–198.
- Brown, I.D. and Altermatt, D. (1985) Bond-valence parameters obtained from a systematic analysis of the Inorganic Crystal Structure Database. *Acta Crystallographica*, B41, 244–247.
- Cruciani, G. (2006) Zeolites upon heating: factors governing their thermal stability and structural changes. *Journal of Physics and Chemistry of Solids*, 67, 1973–1994.
- Evans, H.T. Jr. (1973) The crystal structures of cavansite and pentagonite. *American Mineralogist*, 58, 412–424.
- Ferraris, G. and Ivaldi, G. (1988) Bond valences vs bond length in O–O hydrogen bonds. *Acta Crystallographica*, B44, 341–344.
- Fischer, K.F. (1963) The crystal structure determination of zeolite gismondite $CaAl_2Si_2O_8 \cdot 4H_2O$. *American Mineralogist*, 48, 664–672.
- Frank, H.T., Formoso, M.L.L., Devouard, B., and Gomes, M.E.B. (2005) Cavansite em Morro Reuter, Rio Grande do Sul, Brazil. III Simposio de Vulcanismo e Ambientes Associados (<http://www.museumin.ufrrgs.br/Frank%20et%20al%202005.pdf>).
- Hughes, J.M., Derr, R.S., Cureton, F., Campana, C.F., and Druschel, G. (2011) The crystal structure of cavansite: location of the H_2O molecules and hydrogen atoms in $Ca(VO)(Si_4O_10) \cdot 4H_2O$. *Canadian Mineralogist*, 49, 1267–1272.
- Ishida, N., Kimata, M., Nishida, N., Hatta, T., Shimizu, M., and Akasaka, T. (2009) Polymorphic relation between cavansite and pentagonite: genetic implications of oxonium ion in cavansite. *Journal of Mineralogical and Petrological Science*, 104, 241–252.
- Libowitzky, E. (1999) Correlation of O–H stretching frequencies and O–H hydrogen bond lengths in minerals. *Monatshefte für Chemie*, 130, 1047–1059.
- Milazzo, E., Artioli, G., Gualtieri, A., and Hanson, J.C. (1998) The dehydration process in gismondine: An *in situ* Synchrotron XRPD study. *Proceedings IV Convegno Nazionale Scienza e Tecnologia delle Zeoliti*, 160–165.
- Phadke, A.V. and Apté, A. (1994) Thermal behavior of cavansite from Wagholi, India. *Mineralogical Magazine*, 58, 501–505.
- Powar, K.B. and Byrappa, K. (2001) X-ray, thermal and infrared studies of cavansite from Wagholi western Maharashtra, India. *Journal of Mineralogical and Petrological Science*, 96, 1–6.
- Prasad, P.S.R. and Prasad, S.K. (2007) Dehydration behavior of natural cavansite: an *in-situ* FTIR and Raman spectroscopic study. *Materials Chemistry and Physics*, 105, 395–400.
- Rinaldi, R. and Vezzalini, G. (1985) Gismondine: The detailed X-ray structure refinement of two natural samples. In B. Držaj, S. Hočvar, and S. Pejovnik, Eds., *Zeolites*, p. 481–491. Elsevier, Amsterdam.
- Rinaldi, R., Pluth, J.J., and Smith, J.V. (1975) Crystal structure of cavansite dehydrated at 220°C. *Acta Crystallographica*, B31, 1598–1602.
- Rossmann, G.R. (2011) Mineral spectroscopy server, California Institute of Technology, Pasadena Ca.; <http://minerals.gps.caltech.edu/index.html>; sample GRR 1888 (retrieved 04/20/2012).
- Sheldrick, G.M. (2008) A short history of SHELX. *Acta Crystallographica*, A64, 112–122.
- Solov'ev, M.V., Rastsvetaeva, R.K., and Pushcharovskii, D.Y. (1993) Refined crystal structure of cavansite. *Crystallography Reports*, 38, 274–275.
- Staples, L.W., Evans, H.T. Jr., and Lindsay, J.R. (1973) Cavansite and pentagonite, new dimorphous calcium vanadium silicate minerals from Oregon. *American Mineralogist*, 58, 405–411.
- Thornton, J. (2004) Cavansit aus Neuseeland. *Lapis*, 29(9), 41–42.
- Van Reeuwijk, L.P. (1971) The dehydration of gismondine. *American Mineralogist*, 56, 1655–1659.
- Vezzalini, G., Quartieri, S., and Alberti, A. (1993) Structural modifications induced by dehydration in the zeolite gismondine. *Zeolites*, 13, 34–43.
- Wang, X., Lumei, L., and Jacobson, A.J. (2002) Open-framework and microporous vanadium silicates. *Journal of the American Chemical Society*, 124, 7812–7820.

MANUSCRIPT RECEIVED MAY 14, 2012

MANUSCRIPT ACCEPTED JULY 19, 2012

MANUSCRIPT HANDLED BY G. DIEGO GATTA

Tables 3a–3d for deposit.

TABLE 3a. Anisotropic displacement parameters (\AA^2) for cavansite at RT

Site	U_{11}	U_{22}	U_{33}	U_{23}	U_{13}	U_{12}
V	0.00849(16)	0.00949(16)	0.01330(17)	0	0.00076(11)	0
Ca	0.01036(19)	0.01118(19)	0.0167(2)	0	0.00069(14)	0
Si1	0.00635(17)	0.00920(18)	0.00869(18)	0.00054(13)	– 0.00063(12)	0.00008(13)
Si2	0.00691(17)	0.00834(17)	0.00772(17)	0.00053(12)	0.00091(12)	0.00042(13)
O1	0.0093(5)	0.0098(5)	0.0193(5)	–0.0007(4)	0.0002(4)	–0.0007(4)
O2	0.0154(5)	0.0091(5)	0.0168(5)	0.0015(4)	0.0052(4)	0.0021(4)
O3	0.0122(5)	0.0212(6)	0.0099(5)	0.0039(4)	–0.0014(4)	–0.0003(4)
O4	0.0082(4)	0.0113(5)	0.0172(5)	–0.0015(4)	0.0026(4)	–0.0001(4)
O5	0.0103(5)	0.0122(5)	0.0111(5)	0.0019(4)	–0.0039(4)	–0.0013(4)
O6	0.0231(9)	0.0287(10)	0.0192(8)	0	–0.0052(7)	0
O7	0.0340(9)	0.0489(11)	0.0498(10)	–0.0273(9)	0.0089(7)	0.0048(7)
O8	0.0146(9)	0.0319(11)	0.0658(16)	0	–0.0048(10)	0
O9	0.066(2)	0.109(3)	0.058(2)	0	0.0091(17)	0

Table 3b. Anisotropic displacement parameters (\AA^2) for cavansite at 75 °C

Site	U_{11}	U_{22}	U_{33}	U_{23}	U_{13}	U_{12}
V	0.0098(2)	0.0118(2)	0.0150(2)	0	0.00105(14)	0
Ca	0.0119(2)	0.0135(2)	0.0173(2)	0	0.00026(17)	0
Si1	0.0071(2)	0.0116(2)	0.0104(2)	0.00078(15)	–0.00049(15)	–0.00016(15)
Si2	0.0082(2)	0.0101(2)	0.0097(2)	0.00080(15)	0.00136(15)	0.00053(15)
O1	0.0107(6)	0.0122(6)	0.0220(7)	–0.0010(5)	0.0014(5)	–0.0002(4)
O2	0.0189(6)	0.0110(6)	0.0207(6)	0.0016(5)	0.0079(5)	0.0029(5)
O3	0.0132(6)	0.0262(7)	0.0127(6)	0.0049(5)	–0.0020(5)	–0.0008(5)
O4	0.0098(5)	0.0142(6)	0.0199(6)	–0.0018(5)	0.0039(5)	–0.0005(5)
O5	0.0121(6)	0.0154(6)	0.0138(6)	0.0030(5)	–0.0049(4)	–0.0021(4)
O6	0.0289(12)	0.0370(13)	0.0222(10)	0	–0.0080(9)	0
O8	0.0215(15)	0.099(3)	0.106(4)	0	–0.0007(18)	0

Table 3c. Anisotropic displacement parameters (\AA^2) for cavansite at 175 °C

Site	U_{11}	U_{22}	U_{33}	U_{23}	U_{13}	U_{12}
V	0.0140(2)	0.0168(2)	0.0185(2)	0	0.00103(17)	0
Ca	0.0163(3)	0.0197(3)	0.0194(3)	0	–0.0001(2)	0

Si1	0.0108(2)	0.0170(3)	0.0146(3)	0.00178(17)	-0.00055(18)	0.00016(17)
Si2	0.0124(2)	0.0155(2)	0.0131(2)	0.00137(17)	0.00162(17)	0.00114(18)
O1	0.0153(6)	0.0172(7)	0.0272(8)	-0.0011(6)	0.0017(5)	-0.0002(5)
O2	0.0248(7)	0.0168(7)	0.0237(7)	0.0027(5)	0.0087(6)	0.0043(6)
O3	0.0180(7)	0.0328(9)	0.0169(7)	0.0063(6)	-0.0025(5)	-0.0008(6)
O4	0.0144(7)	0.0194(7)	0.0250(7)	0.0001(5)	0.0050(6)	-0.0003(5)
O5	0.0158(7)	0.0220(7)	0.0190(7)	0.0037(5)	-0.0051(5)	-0.0018(5)
O6	0.0326(13)	0.0404(14)	0.0282(13)	0	-0.0086(11)	0
O8	0.035(2)	0.172(6)	0.157(6)	0	0.029(3)	0

Table 3d. Anisotropic displacement parameters (\AA^2) for cavansite at 350 °C

Site	U_{11}	U_{22}	U_{33}	U_{23}	U_{13}	U_{12}
V	0.0308(12)	0.0317(11)	0.0343(13)	0	0.0063(10)	0
Ca	0.0358(14)	0.0357(14)	0.0405(17)	0	-0.0030(12)	0
Si1	0.0211(12)	0.0300(12)	0.0255(14)	0.0024(9)	-0.0021(9)	0.0000(8)
Si2	0.0241(11)	0.0293(11)	0.0195(13)	0.0015(9)	0.0041(9)	0.0008(9)
O1	0.030(3)	0.033(3)	0.049(4)	0.001(3)	0.002(3)	0.000(2)
O2	0.048(4)	0.032(3)	0.033(4)	0.004(3)	0.016(3)	0.006(3)
O3	0.034(3)	0.054(4)	0.022(3)	0.007(3)	-0.003(3)	-0.002(3)
O4	0.023(3)	0.035(3)	0.035(3)	0.003(2)	0.003(3)	0.000(2)
O5	0.031(3)	0.038(3)	0.024(3)	0.008(2)	-0.004(3)	-0.001(2)
O6	0.067(7)	0.068(7)	0.048(7)	0	-0.010(6)	0

TABLE 5 for deposit

TABLE 5. Interatomic distances (\AA) and T-O-T angles ($^\circ$) of cavansite under ambient conditions and after partial dehydration at 75, 175, and 350 $^\circ\text{C}$

Ca coordination	RT	75 $^\circ\text{C}$	175 $^\circ\text{C}$	350 $^\circ\text{C}$
Ca-O1 (2 \times)	2.3941(11)	2.3726(14)	2.3356(15)	2.292(11)
Ca-O2 (2 \times)	2.4418(12)	2.4081(14)	2.3291(16)	2.271(11)
Ca-O7 (2 \times)	2.3894(16)	2.407(9)	2.402(15)	2.31(5)
Ca-O7a (2 \times)		2.47(1)	2.453(11)	
Ca-O7b (2 \times)		2.409(4)	2.41(2)	2.42(6)
Ca-O8	2.501(2)	2.473(4)	2.402(5)	2.07(8)
Ca-O9	2.834(4)	2.82(3)		
Mean	2.473	2.469*	2.359*	2.260*

*The mean value of the split positions is given.

V coordination	RT	75 $^\circ\text{C}$	175 $^\circ\text{C}$	350 $^\circ\text{C}$
V-O1 (2 \times)	2.0026(11)	2.0032(14)	2.0017(15)	2.01(1)
V-O2 (2 \times)	1.9843(11)	1.9843(14)	1.9718(15)	1.980(9)
V-O6	1.5956(18)	1.590(2)	1.590(3)	1.559(13)
Mean	1.914	1.913	1.907	1.908
Si1 coordination	RT	75 $^\circ\text{C}$	175 $^\circ\text{C}$	350 $^\circ\text{C}$
Si1-O1	1.6027(12)	1.6030(15)	1.6090(16)	1.60(1)
Si1-O3	1.6231(12)	1.6239(15)	1.6220(16)	1.60(1)
Si1-O4	1.6406(11)	1.6357(14)	1.6343(15)	1.620(8)
Si1-O5	1.6298(11)	1.6279(13)	1.6269(15)	1.617(9)
Mean	1.624	1.623	1.623	1.609
Si2 coordination	RT	75 $^\circ\text{C}$	175 $^\circ\text{C}$	350 $^\circ\text{C}$
Si2-O2	1.5922(12)	1.5908(14)	1.5947(16)	1.59(1)
Si2-O3	1.6231(12)	1.6202(14)	1.6233(16)	1.612(9)
Si2-O4	1.6248(11)	1.6283(14)	1.6265(16)	1.625(9)
Si2-O5	1.6234(11)	1.6230(13)	1.6251(15)	1.625(9)
Mean	1.616	1.616	1.617	1.613
T-O-T angles	RT	75 $^\circ\text{C}$	175 $^\circ\text{C}$	350 $^\circ\text{C}$
Si2 O3 Si1	136.36(8)	136.92(9)	135.18(10)	137.3(4)
Si2 O4 Si1	127.78(7)	127.77(9)	127.32(10)	127.0(5)
Si2 O5 Si1	131.42(7)	131.46(9)	128.24(10)	126.2(4)
Mean T-O-T	131.85	132.05	130.25	130.17

TABLE 6 for deposit

TABLE 6. Results of bond valence calculations for cavansite RT, parameters from Brown and Altermatt (1985)

Site	O1	O2	O3	O4	O5	O6	O7	O8	O9	Bvs [#]
V	0.56	0.59				1.67				3.97
			2 × →	2 × →						
Ca	0.28	0.26					0.29	0.23	0.11	2.00
			2 × →	2 × →			2 × →			
Si1	1.06		0.97	0.93	0.95					3.91
Si2		1.04	0.97	0.96	0.97					3.93
H7a						0.8		0.2	1	
								2 × ↓		
H7b				0.2		0.2	0.8			1
H8			0.2				0.8			1
								2 × ↓		
H9a					0.2			0.8	1	
H9b								1*	1	
Bvs [#]					1.92	1.67	0.29	0.23	0.11	
without H										
Bvs [#] with H	1.90	1.89	2.14	1.89	2.12	1.87	1.89	1.83	2.31	

[#] bond valence sum.

*No acceptor was found for H9b.

```

data_cav_rt

_audit_creation_method           SHELLXL-97
_chemical_name_systematic
;
?
;
_chemical_name_common            ?
_chemical_melting_point         ?
_chemical_formula_moiety        ?
_chemical_formula_sum
'H8 Ca O15 Si4 V'
_chemical_formula_weight         451.44

loop_
_atom_type_symbol
_atom_type_description
_atom_type_scat_dispersion_real
_atom_type_scat_dispersion_imag
_atom_type_scat_source
'H'   'H'   0.0000  0.0000
'International Tables Vol C Tables 4.2.6.8 and 6.1.1.4'
'O'   'O'   0.0106  0.0060
'International Tables Vol C Tables 4.2.6.8 and 6.1.1.4'
'Si'   'Si'   0.0817  0.0704
'International Tables Vol C Tables 4.2.6.8 and 6.1.1.4'
'Ca'   'Ca'   0.2262  0.3064
'International Tables Vol C Tables 4.2.6.8 and 6.1.1.4'
'V'   'V'   0.3005  0.5294
'International Tables Vol C Tables 4.2.6.8 and 6.1.1.4'

_symmetry_cell_setting          ?
_symmetry_space_group_name_H-M  ?

loop_
_symmetry_equiv_pos_as_xyz
'x, y, z'
'x+1/2, -y+1/2, -z+1/2'
'-x, y+1/2, -z'
'-x+1/2, -y, z+1/2'
'-x, -y, -z'
'-x-1/2, y-1/2, z-1/2'
'x, -y-1/2, z'
'x-1/2, y, -z-1/2'

_cell_length_a                  9.6329(2)
_cell_length_b                  13.6606(2)
_cell_length_c                  9.7949(2)
_cell_angle_alpha                90.00
_cell_angle_beta                 90.00
_cell_angle_gamma                90.00
_cell_volume                     1288.92(4)
_cell_formula_units_z            4
_cell_measurement_temperature    293(2)

```

```

_cell_measurement_reflns_used      ?
_cell_measurement_theta_min       ?
_cell_measurement_theta_max        ?

_exptl_crystal_description        ?
_exptl_crystal_colour             ?
_exptl_crystal_size_max           ?
_exptl_crystal_size_mid           ?
_exptl_crystal_size_min           ?
_exptl_crystal_density_meas       ?
_exptl_crystal_density_diffrn    2.326
_exptl_crystal_density_method     'not measured'
_exptl_crystal_F_000              908
_exptl_absorpt_coefficient_mu    1.621
_exptl_absorpt_correction_type   ?
_exptl_absorpt_correction_T_min  ?
_exptl_absorpt_correction_T_max  ?
_exptl_absorpt_process_details    ?

_exptl_special_details
;
?
;

_diffrn_ambient_temperature        293(2)
_diffrn_radiation_wavelength       0.71073
_diffrn_radiation_type             MoK\alpha
_diffrn_radiation_source           'fine-focus sealed tube'
_diffrn_radiation_monochromator    graphite
_diffrn_measurement_device_type    ?
_diffrn_measurement_method         ?
_diffrn_detector_area_resol_mean   ?
_diffrn_standards_number           ?
_diffrn_standards_interval_count   ?
_diffrn_standards_interval_time    ?
_diffrn_standards_decay_%          ?
_diffrn_reflns_number              10723
_diffrn_reflns_av_R_equivalents   0.0258
_diffrn_reflns_av_sigmaI/netI     0.0188
_diffrn_reflns_limit_h_min         -13
_diffrn_reflns_limit_h_max         13
_diffrn_reflns_limit_k_min         -19
_diffrn_reflns_limit_k_max         19
_diffrn_reflns_limit_l_min         -13
_diffrn_reflns_limit_l_max         13
_diffrn_reflns_theta_min           2.56
_diffrn_reflns_theta_max           30.50
_reflns_number_total               2039
_reflns_number_gt                 1859
_reflns_threshold_expression       >2\s(I)

_computing_data_collection         ?
_computing_cell_refinement         ?
_computing_data_reduction          ?
_computing_structure_solution      ?

```

```

_computing_structure_refinement      'SHELXL-97 (Sheldrick, 2008)'
_computing_molecular_graphics      ?
_computing_publication_material    ?

_refine_special_details
;
Refinement of F^2^ against ALL reflections. The weighted R-factor wR and
goodness of fit S are based on F^2^, conventional R-factors R are based
on F, with F set to zero for negative F^2^. The threshold expression of
F^2^ > 2\s(F^2^) is used only for calculating R-factors(gt) etc. and is
not relevant to the choice of reflections for refinement. R-factors based
on F^2^ are statistically about twice as large as those based on F, and R-
factors based on ALL data will be even larger.
;

_refine_ls_structure_factor_coef   Fsqd
_refine_ls_matrix_type            full
_refine_ls_weighting_scheme       calc
_refine_ls_weighting_details      'calc w=1/[\s^2^(Fo^2^)+(0.0349P)^2^+1.0944P] where P=(Fo^2^+2Fc^2^)/3'
_atom_sites_solution_primary       direct
_atom_sites_solution_secondary    difmap
_atom_sites_solution_hydrogens    geom
_refine_ls_hydrogen_treatment     mixed
_refine_ls_extinction_method     none
_refine_ls_extinction_coef       ?
_refine_ls_number_reflns         2039
_refine_ls_number_parameters     116
_refine_ls_number_restraints     7
_refine_ls_R_factor_all          0.0262
_refine_ls_R_factor_gt           0.0232
_refine_ls_wR_factor_ref         0.0680
_refine_ls_wR_factor_gt          0.0664
_refine_ls_goodness_of_fit_ref   1.079
_refine_ls_restrained_S_all      1.083
_refine_ls_shift/su_max          0.006
_refine_ls_shift/su_mean         0.000

loop_
_atom_site_label
_atom_site_type_symbol
_atom_site_fract_x
_atom_site_fract_y
_atom_site_fract_z
_atom_site_U_iso_or_equiv
_atom_site_adp_type
_atom_site_occupancy
_atom_site_symmetry_multiplicity
_atom_site_calc_flag
_atom_site_refinement_flags
_atom_site_disorder_assembly
_atom_site_disorder_group
V V 0.02594(4) 0.2500 0.09618(4) 0.01042(9) Uani 1 2 d S . .
Ca Ca -0.38231(4) 0.7500 -0.08263(5) 0.01275(10) Uani 1 2 d S . .
Si1 Si -0.18305(4) 0.53318(3) -0.09496(4) 0.00808(9) Uani 1 1 d . .

```

Si2 Si -0.10728(4) 0.45691(3) 0.18382(4) 0.00766(9) Uani 1 1 d . . .
 O1 O -0.17796(11) 0.65027(8) -0.08597(11) 0.0128(2) Uani 1 1 d . . .
 O2 O -0.08731(12) 0.34231(8) 0.20600(11) 0.0137(2) Uani 1 1 d . . .
 O3 O -0.20339(11) 0.47968(9) 0.05164(11) 0.0144(2) Uani 1 1 d . . .
 O4 O -0.04191(11) 0.48914(8) -0.16578(11) 0.0122(2) Uani 1 1 d . . .
 O5 O -0.31477(11) 0.49541(8) -0.18514(11) 0.0112(2) Uani 1 1 d . . .
 O6 O -0.0430(2) 0.2500 -0.05191(19) 0.0237(4) Uani 1 2 d S . .
 O7 O -0.46993(18) 0.88139(14) 0.05339(19) 0.0442(4) Uani 1 1 d D . .
 H7A H -0.421(3) 0.869(3) 0.136(2) 0.080 Uiso 1 1 d D . .
 H7B H -0.5615(16) 0.891(3) 0.081(4) 0.080 Uiso 1 1 d D . .
 O8 O -0.6383(2) 0.7500 -0.1258(3) 0.0374(5) Uani 1 2 d SD . .
 H8 H -0.685(3) 0.6944(17) -0.093(3) 0.080 Uiso 1 1 d D . .
 O9 O -0.2832(4) 0.7500 0.1898(4) 0.0775(11) Uani 1 2 d SD . .
 H9A H -0.330(5) 0.7500 0.276(3) 0.080 Uiso 1 2 d SD . .
 H9B H -0.192(2) 0.7500 0.230(5) 0.080 Uiso 1 2 d SD . .

loop_

_atom_site_aniso_label
 _atom_site_aniso_U_11
 _atom_site_aniso_U_22
 _atom_site_aniso_U_33
 _atom_site_aniso_U_23
 _atom_site_aniso_U_13
 _atom_site_aniso_U_12

V 0.00849(16) 0.00946(16) 0.01330(17) 0.000 0.00076(11) 0.000
 Ca 0.01036(19) 0.01118(19) 0.0167(2) 0.000 0.00069(14) 0.000
 Si1 0.00635(17) 0.00920(18) 0.00869(18) 0.00054(13) -0.00063(12) 0.00008(13)
 Si2 0.00691(17) 0.00834(17) 0.00772(17) 0.00053(12) 0.00091(12) 0.00042(13)
 O1 0.0093(5) 0.0098(5) 0.0193(5) -0.0007(4) 0.0002(4) -0.0007(4)
 O2 0.0154(5) 0.0091(5) 0.0168(5) 0.0015(4) 0.0052(4) 0.0021(4)
 O3 0.0122(5) 0.0212(6) 0.0099(5) 0.0039(4) -0.0014(4) -0.0003(4)
 O4 0.0082(4) 0.0113(5) 0.0172(5) -0.0015(4) 0.0026(4) -0.0001(4)
 O5 0.0103(5) 0.0122(5) 0.0111(5) 0.0019(4) -0.0039(4) -0.0013(4)
 O6 0.0231(9) 0.0287(10) 0.0192(8) 0.000 -0.0052(7) 0.000
 O7 0.0340(9) 0.0489(11) 0.0498(10) -0.0273(9) 0.0089(7) 0.0048(7)
 O8 0.0146(9) 0.0319(11) 0.0658(16) 0.000 -0.0048(10) 0.000
 O9 0.066(2) 0.109(3) 0.058(2) 0.000 0.0091(17) 0.000

_geom_special_details

;

All s.u.'s (except the s.u. in the dihedral angle between two l.s. planes) are estimated using the full covariance matrix. The cell s.u.'s are taken into account individually in the estimation of s.u.'s in distances, angles and torsion angles; correlations between s.u.'s in cell parameters are only used when they are defined by crystal symmetry. An approximate (isotropic) treatment of cell s.u.'s is used for estimating s.u.'s involving l.s. planes.

;

loop_

_geom_bond_atom_site_label_1
 _geom_bond_atom_site_label_2
 _geom_bond_distance
 _geom_bond_site_symmetry_2
 _geom_bond_publ_flag

V 06 1.5956(18) . ?

V O2 1.9843(11) . ?
V O2 1.9843(11) 7_565 ?
V O1 2.0026(11) 5_565 ?
V O1 2.0026(11) 3_545 ?
V Ca 3.4354(6) 5_565 ?
V Ca 3.4368(6) 6_556 ?
Ca O7 2.3894(16) . ?
Ca O7 2.3894(16) 7_575 ?
Ca O1 2.3941(11) 7_575 ?
Ca O1 2.3941(11) . ?
Ca O2 2.4418(12) 4_464 ?
Ca O2 2.4418(12) 6_565 ?
Ca O8 2.501(2) . ?
Ca O9 2.834(4) . ?
Ca V 3.4354(6) 5_565 ?
Ca V 3.4368(6) 6_565 ?
Ca Si1 3.5315(5) 7_575 ?
Ca Si1 3.5315(5) . ?
Ca H7A 2.71(3) . ?
Si1 O1 1.6027(12) . ?
Si1 O3 1.6231(12) . ?
Si1 O5 1.6298(11) . ?
Si1 O4 1.6406(11) . ?
Si2 O2 1.5922(11) . ?
Si2 O3 1.6217(12) . ?
Si2 O5 1.6234(11) 4_465 ?
Si2 O4 1.6248(11) 5_565 ?
Si2 Ca 3.6377(5) 6_556 ?
O1 V 2.0026(11) 5_565 ?
O2 Ca 2.4418(12) 6_556 ?
O4 Si2 1.6248(11) 5_565 ?
O5 Si2 1.6234(11) 4_464 ?
O7 H7A 0.946(10) . ?
O7 H7B 0.934(10) . ?
O8 H8 0.938(10) . ?
O9 H9A 0.957(10) . ?
O9 H9B 0.961(10) . ?

loop_
 _geom_angle_atom_site_label_1
 _geom_angle_atom_site_label_2
 _geom_angle_atom_site_label_3
 _geom_angle
 _geom_angle_site_symmetry_1
 _geom_angle_site_symmetry_3
 _geom_angle_publ_flag
O6 V O2 105.30(6) . . ?
O6 V O2 105.30(6) . 7_565 ?
O2 V O2 78.92(6) . 7_565 ?
O6 V O1 105.02(6) . 5_565 ?
O2 V O1 89.81(5) . 5_565 ?
O2 V O1 149.48(5) 7_565 5_565 ?
O6 V O1 105.02(6) . 3_545 ?
O2 V O1 149.48(5) . 3_545 ?
O2 V O1 89.81(5) 7_565 3_545 ?

01 V 01 85.73(6) 5_565 3_545 ?
06 V Ca 112.40(7) . 5_565 ?
02 V Ca 124.77(4) . 5_565 ?
02 V Ca 124.77(4) 7_565 5_565 ?
01 V Ca 42.89(3) 5_565 5_565 ?
01 V Ca 42.89(3) 3_545 5_565 ?
06 V Ca 131.65(7) . 6_556 ?
02 V Ca 44.15(3) . 6_556 ?
02 V Ca 44.15(3) 7_565 6_556 ?
01 V Ca 109.88(3) 5_565 6_556 ?
01 V Ca 109.88(3) 3_545 6_556 ?
Ca V Ca 115.954(13) 5_565 6_556 ?
07 Ca 07 97.39(10) . 7_575 ?
07 Ca 01 82.57(5) . 7_575 ?
07 Ca 01 136.51(6) 7_575 7_575 ?
07 Ca 01 136.51(6) . . ?
07 Ca 01 82.57(5) 7_575 . ?
01 Ca 01 69.36(5) 7_575 . ?
07 Ca 02 144.92(6) . 4_464 ?
07 Ca 02 92.44(6) 7_575 4_464 ?
01 Ca 02 112.39(4) 7_575 4_464 ?
01 Ca 02 78.06(4) . 4_464 ?
07 Ca 02 92.44(6) . 6_565 ?
07 Ca 02 144.92(6) 7_575 6_565 ?
01 Ca 02 78.06(4) 7_575 6_565 ?
01 Ca 02 112.39(4) . 6_565 ?
02 Ca 02 62.19(5) 4_464 6_565 ?
07 Ca 08 75.28(6) . . ?
07 Ca 08 75.28(6) 7_575 . ?
01 Ca 08 143.91(3) 7_575 . ?
01 Ca 08 143.91(3) . . ?
02 Ca 08 74.85(6) 4_464 . ?
02 Ca 08 74.85(6) 6_565 . ?
07 Ca 09 66.04(7) . . ?
07 Ca 09 66.04(7) 7_575 . ?
01 Ca 09 74.69(7) 7_575 . ?
01 Ca 09 74.69(7) . . ?
02 Ca 09 147.01(4) 4_464 . ?
02 Ca 09 147.01(4) 6_565 . ?
08 Ca 09 119.40(10) . . ?
07 Ca V 112.00(5) . 5_565 ?
07 Ca V 112.00(5) 7_575 5_565 ?
01 Ca V 34.70(3) 7_575 5_565 ?
01 Ca V 34.70(3) . 5_565 ?
02 Ca V 94.99(3) 4_464 5_565 ?
02 Ca V 94.99(3) 6_565 5_565 ?
08 Ca V 168.06(7) . 5_565 ?
09 Ca V 72.54(8) . 5_565 ?
07 Ca V 111.61(5) . 6_565 ?
07 Ca V 111.61(5) 7_575 6_565 ?
01 Ca V 108.57(3) 7_575 6_565 ?
01 Ca V 108.57(3) . 6_565 ?
02 Ca V 34.47(3) 4_464 6_565 ?
02 Ca V 34.47(3) 6_565 6_565 ?
08 Ca V 56.54(7) . 6_565 ?

09 Ca V 175.94(8) . 6_565 ?
V Ca V 111.526(13) 5_565 6_565 ?
07 Ca Si1 65.23(5) . 7_575 ?
07 Ca Si1 147.26(5) 7_575 7_575 ?
01 Ca Si1 22.39(3) 7_575 7_575 ?
01 Ca Si1 91.71(3) . 7_575 ?
02 Ca Si1 117.99(3) 4_464 7_575 ?
02 Ca Si1 66.61(3) 6_565 7_575 ?
08 Ca Si1 122.001(13) . 7_575 ?
09 Ca Si1 81.33(4) . 7_575 ?
V Ca Si1 57.014(9) 5_565 7_575 ?
V Ca Si1 100.808(11) 6_565 7_575 ?
07 Ca Si1 147.26(5) . . ?
07 Ca Si1 65.23(5) 7_575 . ?
01 Ca Si1 91.71(3) 7_575 . ?
01 Ca Si1 22.39(3) . . ?
02 Ca Si1 66.61(3) 4_464 . ?
02 Ca Si1 117.99(3) 6_565 . ?
08 Ca Si1 122.001(13) . . ?
09 Ca Si1 81.33(4) . . ?
V Ca Si1 57.014(9) 5_565 . ?
V Ca Si1 100.808(11) 6_565 . ?
Si1 Ca Si1 114.006(17) 7_575 . ?
07 Ca H7A 20.1(4) . . ?
07 Ca H7A 87.9(7) 7_575 . ?
01 Ca H7A 77.5(8) 7_575 . ?
01 Ca H7A 117.8(5) . . ?
02 Ca H7A 164.0(5) 4_464 . ?
02 Ca H7A 110.0(6) 6_565 . ?
08 Ca H7A 89.8(6) . . ?
09 Ca H7A 46.0(4) . . ?
V Ca H7A 99.7(7) 5_565 . ?
V Ca H7A 131.7(4) 6_565 . ?
Si1 Ca H7A 66.3(8) 7_575 . ?
Si1 Ca H7A 127.3(4) . . ?
01 Si1 O3 113.86(6) . . ?
01 Si1 O5 111.69(6) . . ?
03 Si1 O5 104.06(6) . . ?
01 Si1 O4 111.34(6) . . ?
03 Si1 O4 108.00(6) . . ?
05 Si1 O4 107.45(6) . . ?
01 Si1 Ca 34.69(4) . . ?
03 Si1 Ca 106.37(5) . . ?
05 Si1 Ca 82.00(4) . . ?
04 Si1 Ca 140.57(4) . . ?
02 Si2 O3 111.50(6) . . ?
02 Si2 O5 110.03(6) . 4_465 ?
03 Si2 O5 106.87(6) . 4_465 ?
02 Si2 O4 110.73(6) . 5_565 ?
03 Si2 O4 109.34(6) . 5_565 ?
05 Si2 O4 108.25(6) 4_465 5_565 ?
02 Si2 Ca 32.17(4) . 6_556 ?
03 Si2 Ca 129.44(5) . 6_556 ?
05 Si2 Ca 78.57(4) 4_465 6_556 ?
04 Si2 Ca 116.44(4) 5_565 6_556 ?

Si1 O1 V 134.31(7) . 5_565 ?
 Si1 O1 Ca 122.92(6) . . ?
 V O1 Ca 102.41(5) 5_565 . ?
 Si2 O2 V 128.12(6) . . ?
 Si2 O2 Ca 127.52(6) . 6_556 ?
 V O2 Ca 101.38(5) . 6_556 ?
 Si2 O3 Si1 136.36(8) . . ?
 Si2 O4 Si1 127.78(7) 5_565 . ?
 Si2 O5 Si1 131.42(7) 4_464 . ?
 Ca O7 H7A 100(2) . . ?
 Ca O7 H7B 127(2) . . ?
 H7A O7 H7B 104(3) . . ?
 Ca O8 H8 114(2) . . ?
 Ca O9 H9A 132(3) . . ?
 Ca O9 H9B 134(3) . . ?
 H9A O9 H9B 94(3) . . ?

loop
 _geom_hbond_atom_site_label_D
 _geom_hbond_atom_site_label_H
 _geom_hbond_atom_site_label_A
 _geom_hbond_distance_DH
 _geom_hbond_distance_HA
 _geom_hbond_distance_DA
 _geom_hbond_angle_DHA
 _geom_hbond_site_symmetry_A
 O9 H9A O6 0.957(10) 2.081(12) 3.033(4) 172(5) 4_465
 O7 H7A O9 0.946(10) 2.17(3) 2.871(4) 130(3) .
 O8 H8 O3 0.938(10) 2.642(13) 3.5634(16) 167(3) 5_465
 O7 H7B O5 0.934(10) 2.11(3) 2.8971(19) 141(3) 3_455

_difffrn_measured_fraction_theta_max	1.000
_difffrn_reflns_theta_full	30.50
_difffrn_measured_fraction_theta_full	1.000
_refine_diff_density_max	0.494
_refine_diff_density_min	-0.572
_refine_diff_density_rms	0.087

```

data_cav_75

_audit_creation_method           SHELXL-97
_chemical_name_systematic
;
?
;
_chemical_name_common            ?
_chemical_melting_point         ?
_chemical_formula_moiety        ?
_chemical_formula_sum
'H8 Ca O15 Si4 V'
_chemical_formula_weight         451.44

loop_
_atom_type_symbol
_atom_type_description
_atom_type_scat_dispersion_real
_atom_type_scat_dispersion_imag
_atom_type_scat_source
'H'   'H'   0.0000  0.0000
'International Tables Vol C Tables 4.2.6.8 and 6.1.1.4'
'O'   'O'   0.0106  0.0060
'International Tables Vol C Tables 4.2.6.8 and 6.1.1.4'
'Si'   'Si'   0.0817  0.0704
'International Tables Vol C Tables 4.2.6.8 and 6.1.1.4'
'Ca'   'Ca'   0.2262  0.3064
'International Tables Vol C Tables 4.2.6.8 and 6.1.1.4'
'V'    'V'    0.3005  0.5294
'International Tables Vol C Tables 4.2.6.8 and 6.1.1.4'

_symmetry_cell_setting          ?
_symmetry_space_group_name_H-M  ?

loop_
_symmetry_equiv_pos_as_xyz
'x, y, z'
'x+1/2, -y+1/2, -z+1/2'
'-x, y+1/2, -z'
'-x+1/2, -y, z+1/2'
'-x, -y, -z'
'-x-1/2, y-1/2, z-1/2'
'x, -y-1/2, z'
'x-1/2, y, -z-1/2'

_cell_length_a                  9.60900(10)
_cell_length_b                  13.6833(2)
_cell_length_c                  9.7559(2)
_cell_angle_alpha                90.00
_cell_angle_beta                 90.00
_cell_angle_gamma                90.00
_cell_volume                     1282.73(3)
_cell_formula_units_z            4
_cell_measurement_temperature    296(2)

```

```

_cell_measurement_reflns_used ?
_cell_measurement_theta_min ?
_cell_measurement_theta_max ?

_exptl_crystal_description ?
_exptl_crystal_colour ?
_exptl_crystal_size_max ?
_exptl_crystal_size_mid ?
_exptl_crystal_size_min ?
_exptl_crystal_density_meas ?
_exptl_crystal_density_diffrn 2.338
_exptl_crystal_density_method 'not measured'
_exptl_crystal_F_000 908
_exptl_absorpt_coefficient_mu 1.629
_exptl_absorpt_correction_type ?
_exptl_absorpt_correction_T_min ?
_exptl_absorpt_correction_T_max ?
_exptl_absorpt_process_details ?

_exptl_special_details
;
?
;

_diffrn_ambient_temperature 296(2)
_diffrn_radiation_wavelength 0.71073
_diffrn_radiation_type MoK\alpha
_diffrn_radiation_source 'fine-focus sealed tube'
_diffrn_radiation_monochromator graphite
_diffrn_measurement_device_type ?
_diffrn_measurement_method ?
_diffrn_detector_area_resol_mean ?
_diffrn_stands_nd_number ?
_diffrn_stands_nd_interval_count ?
_diffrn_stands_nd_interval_time ?
_diffrn_stands_nd_decay_% ?
_diffrn_reflns_number 16172
_diffrn_reflns_av_R_equivalents 0.0280
_diffrn_reflns_av_sigmaI/netI 0.0154
_diffrn_reflns_limit_h_min -13
_diffrn_reflns_limit_h_max 13
_diffrn_reflns_limit_k_min -19
_diffrn_reflns_limit_k_max 19
_diffrn_reflns_limit_l_min -13
_diffrn_reflns_limit_l_max 13
_diffrn_reflns_theta_min 2.56
_diffrn_reflns_theta_max 30.50
_reflns_number_total 2027
_reflns_number_gt 1864
_reflns_threshold_expression >2\s(I)

_computing_data_collection ?
_computing_cell_refinement ?
_computing_data_reduction ?
_computing_structure_solution ?

```

```

_computing_structure_refinement      'SHELXL-97 (Sheldrick, 2008)'
_computing_molecular_graphics      ?
_computing_publication_material    ?

_refine_special_details
;
Refinement of F^2^ against ALL reflections. The weighted R-factor wR and
goodness of fit S are based on F^2^, conventional R-factors R are based
on F, with F set to zero for negative F^2^. The threshold expression of
F^2^ > 2\s(F^2^) is used only for calculating R-factors(gt) etc. and is
not relevant to the choice of reflections for refinement. R-factors based
on F^2^ are statistically about twice as large as those based on F, and R-
factors based on ALL data will be even larger.
;

_refine_ls_structure_factor_coef   Fsqd
_refine_ls_matrix_type            full
_refine_ls_weighting_scheme       calc
_refine_ls_weighting_details      'calc w=1/[s^2^(Fo^2^)+(0.0443P)^2^+2.1038P] where P=(Fo^2^+2Fc^2^)/3'
_atom_sites_solution_primary      direct
_atom_sites_solution_secondary    difmap
_atom_sites_solution_hydrogens    geom
_refine_ls_hydrogen_treatment     mixed
_refine_ls_extinction_method     none
_refine_ls_extinction_coef       ?
_refine_ls_number_reflns         2027
_refine_ls_number_parameters     105
_refine_ls_number_restraints     0
_refine_ls_R_factor_all          0.0323
_refine_ls_R_factor_gt           0.0294
_refine_ls_wR_factor_ref         0.0856
_refine_ls_wR_factor_gt          0.0830
_refine_ls_goodness_of_fit_ref   1.068
_refine_ls_restrained_S_all      1.068
_refine_ls_shift/su_max          0.001
_refine_ls_shift/su_mean         0.000

loop_
_atom_site_label
_atom_site_type_symbol
_atom_site_fract_x
_atom_site_fract_y
_atom_site_fract_z
_atom_site_U_iso_or_equiv
_atom_site_adp_type
_atom_site_occupancy
_atom_site_symmetry_multiplicity
_atom_site_calc_flag
_atom_site_refinement_flags
_atom_site_disorder_assembly
_atom_site_disorder_group
V V 0.02600(5) 0.2500 0.09027(4) 0.01219(11) Uani 1 2 d S . .
Ca Ca -0.38248(5) 0.7500 -0.08753(5) 0.01422(12) Uani 1 2 d S . .
Si1 Si -0.18529(5) 0.53429(4) -0.09246(5) 0.00969(11) Uani 1 1 d . .

```

Si2 Si -0.10434(5) 0.45653(3) 0.18578(5) 0.00934(12) Uani 1 1 d . . .
 O1 O -0.17964(14) 0.65118(10) -0.08307(14) 0.0150(3) Uani 1 1 d . . .
 O2 O -0.08347(15) 0.34199(10) 0.20472(14) 0.0169(3) Uani 1 1 d . . .
 O3 O -0.20289(14) 0.48168(11) 0.05573(14) 0.0174(3) Uani 1 1 d . . .
 O4 O -0.04573(13) 0.49007(10) -0.16576(14) 0.0146(3) Uani 1 1 d . . .
 O5 O -0.31993(13) 0.49792(10) -0.17994(13) 0.0138(3) Uani 1 1 d . . .
 O6 O -0.0455(3) 0.2500 -0.0566(2) 0.0294(5) Uani 1 2 d S . .
 O7 O -0.4471(11) 0.8517(9) 0.1035(13) 0.0448(11) Uiso 0.270(8) 1 d P . .
 O7A O -0.3993(11) 0.8184(8) 0.1464(11) 0.0448(11) Uiso 0.245(7) 1 d P . .
 O7B O -0.4643(5) 0.8806(4) 0.0570(6) 0.0448(11) Uiso 0.557(10) 1 d P . .
 O8 O -0.6396(4) 0.7500 -0.0987(5) 0.0756(14) Uani 1 2 d S . .
 O9 O -0.295(3) 0.7500 0.188(3) 0.0448(11) Uiso 0.105(8) 2 d SP . .

loop_
 _atom_site_aniso_label
 _atom_site_aniso_U_11
 _atom_site_aniso_U_22
 _atom_site_aniso_U_33
 _atom_site_aniso_U_23
 _atom_site_aniso_U_13
 _atom_site_aniso_U_12
 V 0.0098(2) 0.0118(2) 0.0150(2) 0.000 0.00105(14) 0.000
 Ca 0.0119(2) 0.0135(2) 0.0173(2) 0.000 0.00026(17) 0.000
 Si1 0.0071(2) 0.0116(2) 0.0104(2) 0.00078(15) -0.00049(15) -0.00016(15)
 Si2 0.0082(2) 0.0101(2) 0.0097(2) 0.00080(15) 0.00136(15) 0.00053(15)
 O1 0.0107(6) 0.0122(6) 0.0220(7) -0.0010(5) 0.0014(5) -0.0002(4)
 O2 0.0189(6) 0.0110(6) 0.0207(6) 0.0016(5) 0.0079(5) 0.0029(5)
 O3 0.0132(6) 0.0262(7) 0.0127(6) 0.0049(5) -0.0020(5) -0.0008(5)
 O4 0.0098(5) 0.0142(6) 0.0199(6) -0.0018(5) 0.0039(5) -0.0005(5)
 O5 0.0121(6) 0.0154(6) 0.0138(6) 0.0030(5) -0.0049(4) -0.0021(4)
 O6 0.0289(12) 0.0370(13) 0.0222(10) 0.000 -0.0080(9) 0.000
 O8 0.0215(15) 0.099(3) 0.106(4) 0.000 -0.0007(18) 0.000

 _geom_special_details
 ;
 All s.u.'s (except the s.u. in the dihedral angle between two l.s. planes) are estimated using the full covariance matrix. The cell s.u.'s are taken into account individually in the estimation of s.u.'s in distances, angles and torsion angles; correlations between s.u.'s in cell parameters are only used when they are defined by crystal symmetry. An approximate (isotropic) treatment of cell s.u.'s is used for estimating s.u.'s involving l.s. planes.
 ;

 loop_
 _geom_bond_atom_site_label_1
 _geom_bond_atom_site_label_2
 _geom_bond_distance
 _geom_bond_site_symmetry_2
 _geom_bond_publ_flag
 V O6 1.590(2) . ?
 V O2 1.9843(14) . ?
 V O2 1.9843(14) 7_565 ?
 V O1 2.0032(14) 5_565 ?
 V O1 2.0032(14) 3_545 ?
 V Ca 3.4255(7) 5_565 ?

V Ca 3.4325(7) 6_556 ?
 Ca O1 2.3726(14) 7_575 ?
 Ca O1 2.3726(14) . ?
 Ca O7 2.408(9) . ?
 Ca O7 2.408(9) 7_575 ?
 Ca O2 2.4081(14) 4_464 ?
 Ca O2 2.4081(14) 6_565 ?
 Ca O7B 2.409(4) . ?
 Ca O7B 2.409(4) 7_575 ?
 Ca O7A 2.472(10) . ?
 Ca O7A 2.472(10) 7_575 ?
 Ca O8 2.473(4) . ?
 Ca O9 2.82(3) . ?
 Si1 O1 1.6030(15) . ?
 Si1 O3 1.6239(15) . ?
 Si1 O5 1.6279(13) . ?
 Si1 O4 1.6357(14) . ?
 Si2 O2 1.5908(14) . ?
 Si2 O3 1.6202(14) . ?
 Si2 O5 1.6230(13) 4_465 ?
 Si2 O4 1.6283(14) 5_565 ?
 Si2 Ca 3.5907(6) 6_556 ?
 O1 V 2.0032(14) 5_565 ?
 O2 Ca 2.4081(14) 6_556 ?
 O4 Si2 1.6283(14) 5_565 ?
 O5 Si2 1.6230(13) 4_464 ?
 O7 O7B 0.624(12) . ?
 O7 O7A 0.771(14) . ?
 O7A O7B 1.369(12) . ?
 O7A O9 1.43(3) . ?
 O9 O7A 1.43(3) 7_575 ?

loop_
 _geom_angle_atom_site_label_1
 _geom_angle_atom_site_label_2
 _geom_angle_atom_site_label_3
 _geom_angle
 _geom_angle_site_symmetry_1
 _geom_angle_site_symmetry_3
 _geom_angle_publ_flag
 O6 V O2 106.15(9) . . ?
 O6 V O2 106.15(9) . 7_565 ?
 O2 V O2 78.74(8) . 7_565 ?
 O6 V O1 106.68(8) . 5_565 ?
 O2 V O1 88.98(6) . 5_565 ?
 O2 V O1 146.99(6) 7_565 5_565 ?
 O6 V O1 106.68(8) . 3_545 ?
 O2 V O1 146.99(6) . 3_545 ?
 O2 V O1 88.98(6) 7_565 3_545 ?
 O1 V O1 84.91(8) 5_565 3_545 ?
 O6 V Ca 115.18(10) . 5_565 ?
 O2 V Ca 122.31(5) . 5_565 ?
 O2 V Ca 122.31(5) 7_565 5_565 ?
 O1 V Ca 42.50(4) 5_565 5_565 ?
 O1 V Ca 42.50(4) 3_545 5_565 ?

06 V Ca 130.69(10) . 6_556 ?
02 V Ca 43.26(4) . 6_556 ?
02 V Ca 43.26(4) 7_565 6_556 ?
01 V Ca 109.16(4) 5_565 6_556 ?
01 V Ca 109.16(4) 3_545 6_556 ?
Ca V Ca 114.136(15) 5_565 6_556 ?
01 Ca O1 69.49(7) 7_575 . ?
01 Ca O7 82.4(2) 7_575 . ?
01 Ca O7 121.8(3) . . ?
01 Ca O7 121.8(3) 7_575 7_575 ?
01 Ca O7 82.4(2) . 7_575 ?
07 Ca O7 70.7(7) . 7_575 ?
01 Ca O2 115.15(5) 7_575 4_464 ?
01 Ca O2 80.16(5) . 4_464 ?
07 Ca O2 156.7(3) . 4_464 ?
07 Ca O2 108.3(4) 7_575 4_464 ?
01 Ca O2 80.16(5) 7_575 6_565 ?
01 Ca O2 115.15(5) . 6_565 ?
07 Ca O2 108.3(4) . 6_565 ?
07 Ca O2 156.7(3) 7_575 6_565 ?
02 Ca O2 63.02(7) 4_464 6_565 ?
01 Ca O7B 80.47(11) 7_575 . ?
01 Ca O7B 132.87(14) . . ?
07 Ca O7B 14.9(3) . . ?
07 Ca O7B 83.8(4) 7_575 . ?
02 Ca O7B 146.75(14) 4_464 . ?
02 Ca O7B 93.47(16) 6_565 . ?
01 Ca O7B 132.87(14) 7_575 7_575 ?
01 Ca O7B 80.47(11) . 7_575 ?
07 Ca O7B 83.8(4) . 7_575 ?
07 Ca O7B 14.9(3) 7_575 7_575 ?
02 Ca O7B 93.47(16) 4_464 7_575 ?
02 Ca O7B 146.75(14) 6_565 7_575 ?
07B Ca O7B 95.8(3) . 7_575 ?
01 Ca O7A 79.7(2) 7_575 . ?
01 Ca O7A 104.6(3) . . ?
07 Ca O7A 18.1(3) . . ?
07 Ca O7A 59.2(5) 7_575 . ?
02 Ca O7A 165.0(2) 4_464 . ?
02 Ca O7A 124.8(3) 6_565 . ?
07B Ca O7A 32.6(3) . . ?
07B Ca O7A 73.7(3) 7_575 . ?
01 Ca O7A 104.6(3) 7_575 7_575 ?
01 Ca O7A 79.7(2) . 7_575 ?
07 Ca O7A 59.2(5) . 7_575 ?
07 Ca O7A 18.1(3) 7_575 7_575 ?
02 Ca O7A 124.8(3) 4_464 7_575 ?
02 Ca O7A 165.0(2) 6_565 7_575 ?
07B Ca O7A 73.7(3) . 7_575 ?
07B Ca O7A 32.6(3) 7_575 7_575 ?
07A Ca O7A 44.5(5) . 7_575 ?
01 Ca O8 145.24(3) 7_575 . ?
01 Ca O8 145.24(3) . . ?
07 Ca O8 77.1(3) . . ?
07 Ca O8 77.1(3) 7_575 . ?

02 Ca 08 80.04(10) 4_464 . ?
02 Ca 08 80.04(10) 6_565 . ?
07B Ca 08 72.53(13) . . ?
07B Ca 08 72.53(13) 7_575 . ?
07A Ca 08 88.6(3) . . ?
07A Ca 08 88.6(3) 7_575 . ?
01 Ca 09 74.8(5) 7_575 . ?
01 Ca 09 74.8(5) . . ?
07 Ca 09 48.6(5) . . ?
07 Ca 09 48.6(5) 7_575 . ?
02 Ca 09 147.55(15) 4_464 . ?
02 Ca 09 147.55(15) 6_565 . ?
07B Ca 09 62.5(4) . . ?
07B Ca 09 62.5(4) 7_575 . ?
07A Ca 09 30.5(5) . . ?
07A Ca 09 30.5(5) 7_575 . ?
08 Ca 09 109.9(6) . . ?
01 Si1 O3 113.26(8) . . ?
01 Si1 O5 111.22(7) . . ?
03 Si1 O5 104.38(7) . . ?
01 Si1 O4 111.49(7) . . ?
03 Si1 O4 108.10(7) . . ?
05 Si1 O4 108.02(7) . . ?
01 Si1 Ca 34.70(5) . . ?
03 Si1 Ca 107.73(6) . . ?
05 Si1 Ca 80.51(5) . . ?
04 Si1 Ca 139.47(5) . . ?
02 Si2 O3 111.96(8) . . ?
02 Si2 O5 109.94(7) . 4_465 ?
03 Si2 O5 106.76(8) . 4_465 ?
02 Si2 O4 110.15(7) . 5_565 ?
03 Si2 O4 109.17(7) . 5_565 ?
05 Si2 O4 108.75(7) 4_465 5_565 ?
02 Si2 Ca 32.60(5) . 6_556 ?
03 Si2 Ca 128.97(6) . 6_556 ?
05 Si2 Ca 77.84(5) 4_465 6_556 ?
04 Si2 Ca 117.28(5) 5_565 6_556 ?
Si1 O1 V 134.14(8) . 5_565 ?
Si1 O1 Ca 122.67(7) . . ?
V O1 Ca 102.72(6) 5_565 . ?
Si2 O2 V 128.78(8) . . ?
Si2 O2 Ca 126.56(8) . 6_556 ?
V O2 Ca 102.36(6) . 6_556 ?
Si2 O3 Si1 136.92(9) . . ?
Si2 O4 Si1 127.77(9) 5_565 . ?
Si2 O5 Si1 131.46(9) 4_464 . ?
07B O7 O7A 158.0(19) . . ?
07B O7 Ca 82.7(10) . . ?
07A O7 Ca 85.7(11) . . ?
07 O7A O7B 9.8(9) . . ?
07 O7A O9 163.7(19) . . ?
07B O7A O9 155.3(15) . . ?
07 O7A Ca 76.2(11) . . ?
07B O7A Ca 71.2(5) . . ?
09 O7A Ca 88.3(12) . . ?

07 07B 07A 12.2(11) . . ?
07 07B Ca 82.5(10) . . ?
07A 07B Ca 76.3(4) . . ?
07A 09 07A 81.7(18) 7_575 . ?
07A 09 Ca 61.2(12) 7_575 . ?
07A 09 Ca 61.2(12) . . ?

_diffn_measured_fraction_theta_max 0.999
_diffn_reflns_theta_full 30.50
_diffn_measured_fraction_theta_full 0.999
_refine_diff_density_max 0.874
_refine_diff_density_min -0.727
_refine_diff_density_rms 0.102

```

data_cav_175

_audit_creation_method           SHELLXL-97
_chemical_name_systematic
;
?
;
_chemical_name_common            ?
_chemical_melting_point         ?
_chemical_formula_moiety        ?
_chemical_formula_sum
'H3 Ca0.50 O5 Si2 V0.50'
_chemical_formula_weight         184.71

loop_
_atom_type_symbol
_atom_type_description
_atom_type_scat_dispersion_real
_atom_type_scat_dispersion_imag
_atom_type_scat_source
'H'   'H'   0.0000  0.0000
'International Tables Vol C Tables 4.2.6.8 and 6.1.1.4'
'O'   'O'   0.0106  0.0060
'International Tables Vol C Tables 4.2.6.8 and 6.1.1.4'
'Si'   'Si'   0.0817  0.0704
'International Tables Vol C Tables 4.2.6.8 and 6.1.1.4'
'Ca'   'Ca'   0.2262  0.3064
'International Tables Vol C Tables 4.2.6.8 and 6.1.1.4'
'V'   'V'   0.3005  0.5294
'International Tables Vol C Tables 4.2.6.8 and 6.1.1.4'

_symmetry_cell_setting          ?
_symmetry_space_group_name_H-M  ?

loop_
_symmetry_equiv_pos_as_xyz
'x, y, z'
'x+1/2, -y+1/2, -z+1/2'
'-x, y+1/2, -z'
'-x+1/2, -y, z+1/2'
'-x, -y, -z'
'-x-1/2, y-1/2, z-1/2'
'x, -y-1/2, z'
'x-1/2, y, -z-1/2'

_cell_length_a                  9.4746(4)
_cell_length_b                  13.2620(5)
_cell_length_c                  9.6050(4)
_cell_angle_alpha                90.00
_cell_angle_beta                 90.00
_cell_angle_gamma                90.00
_cell_volume                     1206.89(8)
_cell_formula_units_z            8
_cell_measurement_temperature    296(2)

```

_cell_measurement_reflns_used	?
_cell_measurement_theta_min	?
_cell_measurement_theta_max	?
_exptl_crystal_description	?
_exptl_crystal_colour	?
_exptl_crystal_size_max	?
_exptl_crystal_size_mid	?
_exptl_crystal_size_min	?
_exptl_crystal_density_meas	?
_exptl_crystal_density_diffrn	2.033
_exptl_crystal_density_method	'not measured'
_exptl_crystal_F_000	740
_exptl_absorpt_coefficient_mu	1.677
_exptl_absorpt_correction_type	?
_exptl_absorpt_correction_T_min	?
_exptl_absorpt_correction_T_max	?
_exptl_absorpt_process_details	?
_exptl_special_details	
;	
?	
;	
_diffrn_ambient_temperature	296(2)
_diffrn_radiation_wavelength	0.71073
_diffrn_radiation_type	MoK\alpha
_diffrn_radiation_source	'fine-focus sealed tube'
_diffrn_radiation_monochromator	graphite
_diffrn_measurement_device_type	?
_diffrn_measurement_method	?
_diffrn_detector_area_resol_mean	?
_diffrn_standards_number	?
_diffrn_standards_interval_count	?
_diffrn_standards_interval_time	?
_diffrn_standards_decay_%	?
_diffrn_reflns_number	7406
_diffrn_reflns_av_R_equivalents	0.0328
_diffrn_reflns_av_sigmaI/netI	0.0292
_diffrn_reflns_limit_h_min	-12
_diffrn_reflns_limit_h_max	13
_diffrn_reflns_limit_k_min	-18
_diffrn_reflns_limit_k_max	18
_diffrn_reflns_limit_l_min	-7
_diffrn_reflns_limit_l_max	13
_diffrn_reflns_theta_min	2.62
_diffrn_reflns_theta_max	30.50
_reflns_number_total	1900
_reflns_number_gt	1644
_reflns_threshold_expression	>2\s(I)
_computing_data_collection	?
_computing_cell_refinement	?
_computing_data_reduction	?
_computing_structure_solution	?

```

_computing_structure_refinement      'SHELXL-97 (Sheldrick, 2008)'
_computing_molecular_graphics      ?
_computing_publication_material    ?

_refine_special_details
;
Refinement of F^2^ against ALL reflections. The weighted R-factor wR and
goodness of fit S are based on F^2^, conventional R-factors R are based
on F, with F set to zero for negative F^2^. The threshold expression of
F^2^ > 2\s(F^2^) is used only for calculating R-factors(gt) etc. and is
not relevant to the choice of reflections for refinement. R-factors based
on F^2^ are statistically about twice as large as those based on F, and R-
factors based on ALL data will be even larger.
;

_refine_ls_structure_factor_coef   Fsqd
_refine_ls_matrix_type            full
_refine_ls_weighting_scheme       calc
_refine_ls_weighting_details      'calc w=1/[\s^2^(Fo^2^)+(0.0516P)^2^+1.5350P] where P=(Fo^2^+2Fc^2^)/3'
_atom_sites_solution_primary      direct
_atom_sites_solution_secondary    difmap
_atom_sites_solution_hydrogens    geom
_refine_ls_hydrogen_treatment     mixed
_refine_ls_extinction_method     none
_refine_ls_extinction_coef       ?
_refine_ls_number_reflns         1900
_refine_ls_number_parameters     102
_refine_ls_number_restraints     0
_refine_ls_R_factor_all          0.0361
_refine_ls_R_factor_gt           0.0287
_refine_ls_wR_factor_ref         0.0880
_refine_ls_wR_factor_gt          0.0821
_refine_ls_goodness_of_fit_ref   0.964
_refine_ls_restrained_S_all      0.964
_refine_ls_shift/su_max          0.356
_refine_ls_shift/su_mean         0.018

loop_
_atom_site_label
_atom_site_type_symbol
_atom_site_fract_x
_atom_site_fract_y
_atom_site_fract_z
_atom_site_U_iso_or_equiv
_atom_site_adp_type
_atom_site_occupancy
_atom_site_symmetry_multiplicity
_atom_site_calc_flag
_atom_site_refinement_flags
_atom_site_disorder_assembly
_atom_site_disorder_group
V V 0.03479(5) 0.2500 0.09988(5) 0.01642(12) Uani 1 2 d S . .
Ca Ca -0.38889(6) 0.7500 -0.07578(6) 0.01849(14) Uani 1 2 d S . .
Si1 Si -0.19261(6) 0.52653(4) -0.08317(6) 0.01415(13) Uani 1 1 d . .

```

Si2 Si -0.09206(6) 0.46155(4) 0.19910(5) 0.01366(13) Uani 1 1 d . . .
 O1 O -0.18823(15) 0.64770(11) -0.07596(16) 0.0199(3) Uani 1 1 d . . .
 O2 O -0.05978(17) 0.34527(11) 0.22691(16) 0.0218(3) Uani 1 1 d . . .
 O3 O -0.20100(16) 0.47554(13) 0.07010(16) 0.0226(3) Uani 1 1 d . . .
 O4 O -0.05458(16) 0.48034(11) -0.16282(16) 0.0196(3) Uani 1 1 d . . .
 O5 O -0.33434(16) 0.48941(11) -0.16389(15) 0.0189(3) Uani 1 1 d . . .
 O6 O -0.0552(3) 0.2500 -0.0398(3) 0.0337(6) Uani 1 2 d S .
 O7 O -0.430(2) 0.7778(16) 0.1679(16) 0.044(3) Uiso 0.162(12) 1 d P .
 O7A O -0.3625(16) 0.7750(11) 0.1759(12) 0.044(3) Uiso 0.203(10) 1 d P .
 O7B O -0.397(3) 0.810(2) 0.161(2) 0.044(3) Uiso 0.142(14) 1 d P .
 O8 O -0.6409(5) 0.7500 -0.0485(8) 0.121(2) Uani 1 2 d S .

loop_
 _atom_site_aniso_label
 _atom_site_aniso_U_11
 _atom_site_aniso_U_22
 _atom_site_aniso_U_33
 _atom_site_aniso_U_23
 _atom_site_aniso_U_13
 _atom_site_aniso_U_12
 V 0.0140(2) 0.0168(2) 0.0185(2) 0.000 0.00103(17) 0.000
 Ca 0.0163(3) 0.0197(3) 0.0194(3) 0.000 -0.0001(2) 0.000
 Si1 0.0108(2) 0.0170(3) 0.0146(3) 0.00178(17) -0.00055(18) 0.00016(17)
 Si2 0.0124(2) 0.0155(2) 0.0131(2) 0.00137(17) 0.00162(17) 0.00114(18)
 O1 0.0153(6) 0.0172(7) 0.0272(8) -0.0011(6) 0.0017(5) -0.0002(5)
 O2 0.0248(7) 0.0168(7) 0.0237(7) 0.0027(5) 0.0087(6) 0.0043(6)
 O3 0.0180(7) 0.0328(9) 0.0169(7) 0.0063(6) -0.0025(5) -0.0008(6)
 O4 0.0144(7) 0.0194(7) 0.0250(7) 0.0001(5) 0.0050(6) -0.0003(5)
 O5 0.0158(7) 0.0220(7) 0.0190(7) 0.0037(5) -0.0051(5) -0.0018(5)
 O6 0.0326(13) 0.0404(14) 0.0282(13) 0.000 -0.0086(11) 0.000
 O8 0.035(2) 0.172(6) 0.157(6) 0.000 0.029(3) 0.000

 _geom_special_details
 ;
 All s.u.'s (except the s.u. in the dihedral angle between two l.s. planes) are estimated using the full covariance matrix. The cell s.u.'s are taken into account individually in the estimation of s.u.'s in distances, angles and torsion angles; correlations between s.u.'s in cell parameters are only used when they are defined by crystal symmetry. An approximate (isotropic) treatment of cell s.u.'s is used for estimating s.u.'s involving l.s. planes.

loop_
 _geom_bond_atom_site_label_1
 _geom_bond_atom_site_label_2
 _geom_bond_distance
 _geom_bond_site_symmetry_2
 _geom_bond_publ_flag
 V 06 1.590(3) . ?
 V 02 1.9718(15) 7_565 ?
 V 02 1.9718(15) . ?
 V 01 2.0017(15) 5_565 ?
 V 01 2.0017(15) 3_545 ?
 V Ca 3.3629(8) 5_565 ?
 V Ca 3.4082(8) 6_556 ?

Ca O7B 2.415(19) . ?
 Ca O7B 2.415(19) 7_575 ?
 Ca O2 2.3291(16) 4_464 ?
 Ca O2 2.3291(16) 6_565 ?
 Ca O1 2.3356(15) 7_575 ?
 Ca O1 2.3356(15) . ?
 Ca O7 2.402(15) . ?
 Ca O7 2.402(15) 7_575 ?
 Ca O8 2.402(5) . ?
 Ca O7A 2.453(11) . ?
 Ca O7A 2.453(11) 7_575 ?
 Ca V 3.3629(8) 5_565 ?
 Si1 O1 1.6090(16) . ?
 Si1 O3 1.6220(16) . ?
 Si1 O5 1.6269(15) . ?
 Si1 O4 1.6343(15) . ?
 Si2 O2 1.5947(16) . ?
 Si2 O3 1.6233(16) . ?
 Si2 O5 1.6251(15) 4_465 ?
 Si2 O4 1.6265(16) 5_565 ?
 Si2 Ca 3.5468(6) 6_556 ?
 O1 V 2.0017(15) 5_565 ?
 O2 Ca 2.3291(16) 6_556 ?
 O4 Si2 1.6265(15) 5_565 ?
 O5 Si2 1.6251(15) 4_464 ?
 O7 O7A 0.65(2) . ?
 O7 O7B 0.53(2) . ?
 O7 O7 0.74(4) 7_575 ?
 O7 O7A 0.954(17) 7_575 ?
 O7 O7B 1.21(4) 7_575 ?
 O7A O7A 0.66(3) 7_575 ?
 O7A O7 0.954(17) 7_575 ?
 O7A O7B 0.58(2) . ?
 O7A O7B 1.18(4) 7_575 ?
 O7B O7 1.21(4) 7_575 ?
 O7B O7A 1.18(4) 7_575 ?

loop_
 _geom_angle_atom_site_label_1
 _geom_angle_atom_site_label_2
 _geom_angle_atom_site_label_3
 _geom_angle
 _geom_angle_site_symmetry_1
 _geom_angle_site_symmetry_3
 _geom_angle_publ_flag
 O6 V O2 106.17(9) . 7_565 ?
 O6 V O2 106.17(9) . . ?
 O2 V O2 79.70(9) 7_565 . ?
 O6 V O1 107.02(9) . 5_565 ?
 O2 V O1 146.65(7) 7_565 5_565 ?
 O2 V O1 88.10(6) . 5_565 ?
 O6 V O1 107.02(9) . 3_545 ?
 O2 V O1 88.10(6) 7_565 3_545 ?
 O2 V O1 146.65(7) . 3_545 ?
 O1 V O1 85.34(9) 5_565 3_545 ?

06 V Ca 118.49(10) . 5_565 ?
02 V Ca 119.73(5) 7_565 5_565 ?
02 V Ca 119.73(5) . 5_565 ?
01 V Ca 42.91(4) 5_565 5_565 ?
01 V Ca 42.91(4) 3_545 5_565 ?
06 V Ca 123.63(11) . 6_556 ?
02 V Ca 41.42(4) 7_565 6_556 ?
02 V Ca 41.42(4) . 6_556 ?
01 V Ca 113.55(5) 5_565 6_556 ?
01 V Ca 113.55(5) 3_545 6_556 ?
Ca V Ca 117.876(18) 5_565 6_556 ?
07B Ca 07B 38.4(15) . 7_575 ?
07B Ca 02 160.0(7) . 4_464 ?
07B Ca 02 125.6(7) 7_575 4_464 ?
07B Ca 02 125.6(7) . 6_565 ?
07B Ca 02 160.0(7) 7_575 6_565 ?
02 Ca 02 65.71(8) 4_464 6_565 ?
07B Ca 01 80.6(7) . 7_575 ?
07B Ca 01 102.6(6) 7_575 7_575 ?
02 Ca 01 118.98(6) 4_464 7_575 ?
02 Ca 01 81.62(5) 6_565 7_575 ?
07B Ca 01 102.6(6) . . ?
07B Ca 01 80.6(7) 7_575 . ?
02 Ca 01 81.62(5) 4_464 . ?
02 Ca 01 118.98(6) 6_565 . ?
01 Ca 01 71.02(7) 7_575 . ?
07B Ca 07 12.7(5) . . ?
07B Ca 07 29.0(11) 7_575 . ?
02 Ca 07 147.3(6) 4_464 . ?
02 Ca 07 132.5(4) 6_565 . ?
01 Ca 07 92.6(6) 7_575 . ?
01 Ca 07 102.9(4) . . ?
07B Ca 07 29.0(11) . 7_575 ?
07B Ca 07 12.7(5) 7_575 7_575 ?
02 Ca 07 132.5(4) 4_464 7_575 ?
02 Ca 07 147.3(6) 6_565 7_575 ?
01 Ca 07 102.9(4) 7_575 7_575 ?
01 Ca 07 92.6(6) . 7_575 ?
07 Ca 07 17.7(10) . 7_575 ?
07B Ca 08 82.2(6) . . ?
07B Ca 08 82.2(6) 7_575 . ?
02 Ca 08 83.17(16) 4_464 . ?
02 Ca 08 83.17(16) 6_565 . ?
01 Ca 08 144.02(5) 7_575 . ?
01 Ca 08 144.02(5) . . ?
07 Ca 08 74.4(5) . . ?
07 Ca 08 74.4(5) 7_575 . ?
07B Ca 07A 13.8(5) . . ?
07B Ca 07A 28.1(9) 7_575 . ?
02 Ca 07A 153.7(3) 4_464 . ?
02 Ca 07A 138.6(4) 6_565 . ?
01 Ca 07A 80.8(3) 7_575 . ?
01 Ca 07A 89.8(4) . . ?
07 Ca 07A 15.3(5) . . ?
07 Ca 07A 22.6(4) 7_575 . ?

08 Ca 07A 89.7(4) . . ?
07B Ca 07A 28.1(9) . 7_575 ?
07B Ca 07A 13.8(5) 7_575 7_575 ?
02 Ca 07A 138.6(4) 4_464 7_575 ?
02 Ca 07A 153.7(3) 6_565 7_575 ?
01 Ca 07A 89.8(4) 7_575 7_575 ?
01 Ca 07A 80.8(3) . 7_575 ?
07 Ca 07A 22.6(4) . 7_575 ?
07 Ca 07A 15.3(5) 7_575 7_575 ?
08 Ca 07A 89.7(4) . 7_575 ?
07A Ca 07A 15.5(7) . 7_575 ?
07B Ca V 95.6(6) . 5_565 ?
07B Ca V 95.6(6) 7_575 5_565 ?
02 Ca V 98.76(4) 4_464 5_565 ?
02 Ca V 98.76(4) 6_565 5_565 ?
01 Ca V 35.70(4) 7_575 5_565 ?
01 Ca V 35.70(4) . 5_565 ?
07 Ca V 103.3(5) . 5_565 ?
07 Ca V 103.3(5) 7_575 5_565 ?
08 Ca V 177.69(18) . 5_565 ?
07A Ca V 88.1(3) . 5_565 ?
07A Ca V 88.1(3) 7_575 5_565 ?
01 Si1 O3 112.25(9) . . ?
01 Si1 O5 110.12(8) . . ?
03 Si1 O5 105.42(8) . . ?
01 Si1 O4 111.96(8) . . ?
03 Si1 O4 107.93(8) . . ?
05 Si1 O4 108.90(8) . . ?
01 Si1 Ca 33.59(5) . . ?
03 Si1 Ca 107.98(6) . . ?
05 Si1 Ca 80.06(6) . . ?
04 Si1 Ca 138.78(6) . . ?
02 Si2 O3 111.12(9) . . ?
02 Si2 O5 109.49(8) . 4_465 ?
03 Si2 O5 107.43(8) . 4_465 ?
02 Si2 O4 109.28(8) . 5_565 ?
03 Si2 O4 108.99(8) . 5_565 ?
05 Si2 O4 110.51(8) 4_465 5_565 ?
02 Si2 Ca 30.98(6) . 6_556 ?
03 Si2 Ca 121.56(6) . 6_556 ?
05 Si2 Ca 78.52(6) 4_465 6_556 ?
04 Si2 Ca 123.29(6) 5_565 6_556 ?
Si1 O1 V 133.68(9) . 5_565 ?
Si1 O1 Ca 124.00(8) . . ?
V O1 Ca 101.40(6) 5_565 . ?
Si2 O2 V 127.10(9) . . ?
Si2 O2 Ca 128.38(8) . 6_556 ?
V O2 Ca 104.52(6) . 6_556 ?
Si1 O3 Si2 135.18(10) . . ?
Si2 O4 Si1 127.32(10) 5_565 . ?
Si2 O5 Si1 128.24(10) 4_464 . ?
07A O7 O7B 58(3) . . ?
07A O7 O7 87(2) . 7_575 ?
07B O7 O7 143(4) . 7_575 ?
07A O7 O7A 44(2) . 7_575 ?

07B 07 07A 101(4) . 7_575 ?
 07 07 07A 42.8(17) 7_575 7_575 ?
 07A 07 07B 72(3) . 7_575 ?
 07B 07 07B 127(5) . 7_575 ?
 07 07 07B 15.5(15) 7_575 7_575 ?
 07A 07 07B 28.4(14) 7_575 7_575 ?
 07A 07 Ca 86.8(18) . . ?
 07B 07 Ca 85(3) . . ?
 07 07 Ca 81.2(5) 7_575 . ?
 07A 07 Ca 81.7(12) 7_575 . ?
 07B 07 Ca 76.1(13) 7_575 . ?
 07 07A 07A 93(2) . 7_575 ?
 07 07A 07 51(3) . 7_575 ?
 07A 07A 07 42.8(17) 7_575 7_575 ?
 07 07A 07B 51(2) . . ?
 07A 07A 07B 142(3) 7_575 . ?
 07 07A 07B 101(4) 7_575 . ?
 07 07A 07B 76(3) . 7_575 ?
 07A 07A 07B 17.6(14) 7_575 7_575 ?
 07 07A 07B 26.3(14) 7_575 7_575 ?
 07B 07A 07B 125(4) . 7_575 ?
 07 07A Ca 77.9(17) . . ?
 07A 07A Ca 82.2(3) 7_575 . ?
 07 07A Ca 75.7(12) 7_575 . ?
 07B 07A Ca 79(2) . . ?
 07B 07A Ca 74.2(11) 7_575 . ?
 07 07B 07A 71(4) . . ?
 07 07B 07 22(2) . 7_575 ?
 07A 07B 07 51(3) . 7_575 ?
 07 07B 07A 52(3) . 7_575 ?
 07A 07B 07A 20.0(18) . 7_575 ?
 07 07B 07A 31.6(18) 7_575 7_575 ?
 07 07B Ca 82(3) . . ?
 07A 07B Ca 87(2) . . ?
 07 07B Ca 74.9(14) 7_575 . ?
 07A 07B Ca 77.8(13) 7_575 . ?

_diffrn_measured_fraction_theta_max	0.994
_diffrn_reflns_theta_full	30.50
_diffrn_measured_fraction_theta_full	0.994
_refine_diff_density_max	0.614
_refine_diff_density_min	-0.548
_refine_diff_density_rms	0.095

```

data_cav_350

_audit_creation_method           SHELLXL-97
_chemical_name_systematic
;
?
;
_chemical_name_common            ?
_chemical_melting_point          ?
_chemical_formula_moiety         ?
_chemical_formula_sum
'H1.50 Ca0.50 O5 Si2 V0.50'
_chemical_formula_weight          183.20

loop_
_atom_type_symbol
_atom_type_description
_atom_type_scat_dispersion_real
_atom_type_scat_dispersion_imag
_atom_type_scat_source
'H'   'H'   0.0000  0.0000
'International Tables Vol C Tables 4.2.6.8 and 6.1.1.4'
'O'   'O'   0.0106  0.0060
'International Tables Vol C Tables 4.2.6.8 and 6.1.1.4'
'Si'   'Si'   0.0817  0.0704
'International Tables Vol C Tables 4.2.6.8 and 6.1.1.4'
'Ca'   'Ca'   0.2262  0.3064
'International Tables Vol C Tables 4.2.6.8 and 6.1.1.4'
'V'    'V'    0.3005  0.5294
'International Tables Vol C Tables 4.2.6.8 and 6.1.1.4'

_symmetry_cell_setting          ?
_symmetry_space_group_name_H-M   ?

loop_
_symmetry_equiv_pos_as_xyz
'x, y, z'
'x+1/2, -y+1/2, -z+1/2'
'-x, y+1/2, -z'
'-x+1/2, -y, z+1/2'
'-x, -y, -z'
'-x-1/2, y-1/2, z-1/2'
'x, -y-1/2, z'
'x-1/2, y, -z-1/2'

_cell_length_a                  9.39(5)
_cell_length_b                  13.11(8)
_cell_length_c                  9.39(5)
_cell_angle_alpha                90.00
_cell_angle_beta                 90.00
_cell_angle_gamma                90.00
_cell_volume                     1156(11)
_cell_formula_units_z             8
_cell_measurement_temperature     296(2)

```

```

_cell_measurement_reflns_used      ?
_cell_measurement_theta_min       ?
_cell_measurement_theta_max        ?

_exptl_crystal_description        ?
_exptl_crystal_colour             ?
_exptl_crystal_size_max           ?
_exptl_crystal_size_mid           ?
_exptl_crystal_size_min           ?
_exptl_crystal_density_meas       ?
_exptl_crystal_density_diffrn    2.105
_exptl_crystal_density_method     'not measured'
_exptl_crystal_F_000              728
_exptl_absorpt_coefficient_mu    1.749
_exptl_absorpt_correction_type   ?
_exptl_absorpt_correction_T_min  ?
_exptl_absorpt_correction_T_max  ?
_exptl_absorpt_process_details    ?

_exptl_special_details
;
?
;

_diffrn_ambient_temperature        296(2)
_diffrn_radiation_wavelength       0.71073
_diffrn_radiation_type             MoK\alpha
_diffrn_radiation_source           'fine-focus sealed tube'
_diffrn_radiation_monochromator    graphite
_diffrn_measurement_device_type    ?
_diffrn_measurement_method         ?
_diffrn_detector_area_resol_mean   ?
_diffrn_standards_number           ?
_diffrn_standards_interval_count   ?
_diffrn_standards_interval_time    ?
_diffrn_standards_decay_%          ?
_diffrn_reflns_number              4845
_diffrn_reflns_av_R_equivalents   0.0531
_diffrn_reflns_av_sigmaI/netI     0.0382
_diffrn_reflns_limit_h_min         -10
_diffrn_reflns_limit_h_max         10
_diffrn_reflns_limit_k_min         -14
_diffrn_reflns_limit_k_max         14
_diffrn_reflns_limit_l_min         -10
_diffrn_reflns_limit_l_max         10
_diffrn_reflns_theta_min           2.67
_diffrn_reflns_theta_max           23.85
_reflns_number_total               916
_reflns_number_gt                 731
_reflns_threshold_expression       >2\s(I)

_computing_data_collection         ?
_computing_cell_refinement         ?
_computing_data_reduction          ?
_computing_structure_solution      ?

```

```

_computing_structure_refinement      'SHELXL-97 (Sheldrick, 2008)'
_computing_molecular_graphics      ?
_computing_publication_material    ?

_refine_special_details
;
Refinement of F^2^ against ALL reflections. The weighted R-factor wR and
goodness of fit S are based on F^2^, conventional R-factors R are based
on F, with F set to zero for negative F^2^. The threshold expression of
F^2^ > 2\s(F^2^) is used only for calculating R-factors(gt) etc. and is
not relevant to the choice of reflections for refinement. R-factors based
on F^2^ are statistically about twice as large as those based on F, and R-
factors based on ALL data will be even larger.
;

_refine_ls_structure_factor_coef   Fsqd
_refine_ls_matrix_type            full
_refine_ls_weighting_scheme       calc
_refine_ls_weighting_details      'calc w=1/[\s^2^(Fo^2^)+(0.1015P)^2^+5.6836P] where P=(Fo^2^+2Fc^2^)/3'
_atom_sites_solution_primary       direct
_atom_sites_solution_secondary    difmap
_atom_sites_solution_hydrogens    geom
_refine_ls_hydrogen_treatment     mixed
_refine_ls_extinction_method     none
_refine_ls_extinction_coef       ?
_refine_ls_number_reflns         916
_refine_ls_number_parameters     95
_refine_ls_number_restraints     0
_refine_ls_R_factor_all          0.0783
_refine_ls_R_factor_gt           0.0593
_refine_ls_wR_factor_ref         0.1833
_refine_ls_wR_factor_gt          0.1683
_refine_ls_goodness_of_fit_ref   1.149
_refine_ls_restrained_S_all      1.149
_refine_ls_shift/su_max          0.000
_refine_ls_shift/su_mean         0.000

loop_
_atom_site_label
_atom_site_type_symbol
_atom_site_fract_x
_atom_site_fract_y
_atom_site_fract_z
_atom_site_U_iso_or_equiv
_atom_site_adp_type
_atom_site_occupancy
_atom_site_symmetry_multiplicity
_atom_site_calc_flag
_atom_site_refinement_flags
_atom_site_disorder_assembly
_atom_site_disorder_group
V V 0.0374(2) 0.2500 0.0993(2) 0.0323(6) Uani 1 2 d S . .
Ca Ca -0.3884(3) 0.7500 -0.0715(3) 0.0373(8) Uani 1 2 d S . .
Si1 Si -0.1968(2) 0.52399(16) -0.0781(2) 0.0256(6) Uani 1 1 d . .

```

Si2 Si -0.0833(2) 0.46265(16) 0.2073(2) 0.0243(6) Uani 1 1 d . . .
 O1 O -0.1921(6) 0.6461(4) -0.0706(7) 0.0373(15) Uani 1 1 d . . .
 O2 O -0.0485(6) 0.3461(4) 0.2374(6) 0.0378(15) Uani 1 1 d . . .
 O3 O -0.1946(6) 0.4739(5) 0.0777(6) 0.0366(15) Uani 1 1 d . . .
 O4 O -0.0631(5) 0.4784(4) -0.1666(6) 0.0309(14) Uani 1 1 d . . .
 O5 O -0.3434(6) 0.4873(4) -0.1524(6) 0.0310(14) Uani 1 1 d . . .
 O6 O -0.0568(12) 0.2500 -0.0373(12) 0.061(3) Uani 1 2 d S . .
 O7 O -0.517(6) 0.780(4) 0.134(6) 0.129(18) Uiso 0.25(3) 1 d P . .
 O7B O -0.415(7) 0.782(4) 0.181(6) 0.129(18) Uiso 0.22(3) 1 d P . .
 O8 O -0.590(9) 0.7500 0.018(10) 0.129(18) Uiso 0.24(4) 2 d SP . .

loop_
 _atom_site_aniso_label
 _atom_site_aniso_U_11
 _atom_site_aniso_U_22
 _atom_site_aniso_U_33
 _atom_site_aniso_U_23
 _atom_site_aniso_U_13
 _atom_site_aniso_U_12
 V 0.0308(12) 0.0317(11) 0.0343(13) 0.000 0.0063(10) 0.000
 Ca 0.0358(14) 0.0357(14) 0.0405(17) 0.000 -0.0030(12) 0.000
 Si1 0.0211(12) 0.0300(12) 0.0255(14) 0.0024(9) -0.0021(9) 0.0000(8)
 Si2 0.0241(11) 0.0293(11) 0.0195(13) 0.0015(9) 0.0041(9) 0.0008(9)
 O1 0.030(3) 0.033(3) 0.049(4) 0.001(3) 0.002(3) 0.000(2)
 O2 0.048(4) 0.032(3) 0.033(4) 0.004(3) 0.016(3) 0.006(3)
 O3 0.034(3) 0.054(4) 0.022(3) 0.007(3) -0.003(3) -0.002(3)
 O4 0.023(3) 0.035(3) 0.035(3) 0.003(2) 0.003(3) 0.000(2)
 O5 0.031(3) 0.038(3) 0.024(3) 0.008(2) -0.004(3) -0.001(2)
 O6 0.067(7) 0.068(7) 0.048(7) 0.000 -0.010(6) 0.000

_geom_special_details

;

All s.u.'s (except the s.u. in the dihedral angle between two l.s. planes) are estimated using the full covariance matrix. The cell s.u.'s are taken into account individually in the estimation of s.u.'s in distances, angles and torsion angles; correlations between s.u.'s in cell parameters are only used when they are defined by crystal symmetry. An approximate (isotropic) treatment of cell s.u.'s is used for estimating s.u.'s involving l.s. planes.

;

loop_
 _geom_bond_atom_site_label_1
 _geom_bond_atom_site_label_2
 _geom_bond_distance
 _geom_bond_site_symmetry_2
 _geom_bond_publ_flag
 V O6 1.559(13) . ?
 V O2 1.980(9) . ?
 V O2 1.980(9) 7_565 ?
 V O1 2.009(10) 5_565 ?
 V O1 2.009(10) 3_545 ?
 V Ca 3.306(19) 5_565 ?
 V Ca 3.394(17) 6_556 ?
 Ca O8 2.07(8) . ?
 Ca O2 2.271(11) 4_464 ?

Ca O2 2.271(11) 6_565 ?
 Ca O1 2.292(11) 7_575 ?
 Ca O1 2.292(11) . ?
 Ca O7 2.31(5) . ?
 Ca O7 2.31(5) 7_575 ?
 Ca O7B 2.42(6) . ?
 Ca O7B 2.42(6) 7_575 ?
 Ca V 3.306(19) 5_565 ?
 Ca V 3.394(17) 6_565 ?
 Ca Si1 3.467(16) 7_575 ?
 Si1 O1 1.603(11) . ?
 Si1 O3 1.603(10) . ?
 Si1 O5 1.617(9) . ?
 Si1 O4 1.620(8) . ?
 Si2 O2 1.588(10) . ?
 Si2 O3 1.612(9) . ?
 Si2 O4 1.623(9) 5_565 ?
 Si2 O5 1.625(9) 4_465 ?
 Si2 Ca 3.486(15) 6_556 ?
 O1 V 2.009(10) 5_565 ?
 O2 Ca 2.271(11) 6_556 ?
 O4 Si2 1.623(9) 5_565 ?
 O5 Si2 1.625(9) 4_464 ?
 O7 O7 0.79(10) 7_575 ?
 O7 O7B 1.05(6) . ?
 O7 O7B 1.33(6) 7_575 ?
 O7 O8 1.34(9) . ?
 O7B O7B 0.83(11) 7_575 ?
 O7B O7 1.33(6) 7_575 ?
 O8 O7 1.34(9) 7_575 ?

loop_
 _geom_angle_atom_site_label_1
 _geom_angle_atom_site_label_2
 _geom_angle_atom_site_label_3
 _geom_angle
 _geom_angle_site_symmetry_1
 _geom_angle_site_symmetry_3
 _geom_angle_publ_flag
 O6 V O2 108.0(5) . . ?
 O6 V O2 108.0(5) . 7_565 ?
 O2 V O2 79.0(5) . 7_565 ?
 O6 V O1 107.4(4) . 5_565 ?
 O2 V O1 87.2(4) . 5_565 ?
 O2 V O1 144.5(3) 7_565 5_565 ?
 O6 V O1 107.4(4) . 3_545 ?
 O2 V O1 144.5(3) . 3_545 ?
 O2 V O1 87.2(4) 7_565 3_545 ?
 O1 V O1 85.3(6) 5_565 3_545 ?
 O6 V Ca 120.0(5) . 5_565 ?
 O2 V Ca 117.3(2) . 5_565 ?
 O2 V Ca 117.3(2) 7_565 5_565 ?
 O1 V Ca 43.0(3) 5_565 5_565 ?
 O1 V Ca 43.0(3) 3_545 5_565 ?
 O6 V Ca 121.1(6) . 6_556 ?

O2 V Ca 40.1(3) . 6_556 ?
O2 V Ca 40.1(3) 7_565 6_556 ?
O1 V Ca 114.9(2) 5_565 6_556 ?
O1 V Ca 114.9(2) 3_545 6_556 ?
Ca V Ca 118.88(16) 5_565 6_556 ?
O8 Ca O2 95(2) . 4_464 ?
O8 Ca O2 95(2) . 6_565 ?
O2 Ca O2 67.4(5) 4_464 6_565 ?
O8 Ca O1 137.1(13) . 7_575 ?
O2 Ca O1 122.9(3) 4_464 7_575 ?
O2 Ca O1 83.3(3) 6_565 7_575 ?
O8 Ca O1 137.1(13) . . ?
O2 Ca O1 83.3(3) 4_464 . ?
O2 Ca O1 122.9(3) 6_565 . ?
O1 Ca O1 72.9(5) 7_575 . ?
O8 Ca O7 35(2) . . ?
O2 Ca O7 128.2(16) 4_464 . ?
O2 Ca O7 115.4(15) 6_565 . ?
O1 Ca O7 108.4(15) 7_575 . ?
O1 Ca O7 121.2(15) . . ?
O8 Ca O7 35(2) . 7_575 ?
O2 Ca O7 115.4(15) 4_464 7_575 ?
O2 Ca O7 128.2(16) 6_565 7_575 ?
O1 Ca O7 121.2(15) 7_575 7_575 ?
O1 Ca O7 108.4(15) . 7_575 ?
O7 Ca O7 20(3) . 7_575 ?
O8 Ca O7B 60(3) . . ?
O2 Ca O7B 147.4(15) 4_464 . ?
O2 Ca O7B 130.7(15) 6_565 . ?
O1 Ca O7B 88.7(15) 7_575 . ?
O1 Ca O7B 100.4(15) . . ?
O7 Ca O7B 25.6(15) . . ?
O7 Ca O7B 32.6(16) 7_575 . ?
O8 Ca O7B 60(3) . 7_575 ?
O2 Ca O7B 130.7(14) 4_464 7_575 ?
O2 Ca O7B 147.4(15) 6_565 7_575 ?
O1 Ca O7B 100.4(15) 7_575 7_575 ?
O1 Ca O7B 88.7(15) . 7_575 ?
O7 Ca O7B 32.6(16) . 7_575 ?
O7 Ca O7B 25.6(15) 7_575 7_575 ?
O7B Ca O7B 20(3) . 7_575 ?
O8 Ca V 160(3) . 5_565 ?
O2 Ca V 101.4(2) 4_464 5_565 ?
O2 Ca V 101.4(2) 6_565 5_565 ?
O1 Ca V 36.7(3) 7_575 5_565 ?
O1 Ca V 36.7(3) . 5_565 ?
O7 Ca V 125.9(17) . 5_565 ?
O7 Ca V 125.9(17) 7_575 5_565 ?
O7B Ca V 100.4(16) . 5_565 ?
O7B Ca V 100.4(16) 7_575 5_565 ?
O8 Ca V 90(3) . 6_565 ?
O2 Ca V 34.2(2) 4_464 6_565 ?
O2 Ca V 34.2(2) 6_565 6_565 ?
O1 Ca V 109.6(2) 7_575 6_565 ?
O1 Ca V 109.6(2) . 6_565 ?

07 Ca V 123.1(17) . 6_565 ?
07 Ca V 123.1(17) 7_575 6_565 ?
07B Ca V 148.2(16) . 6_565 ?
07B Ca V 148.2(16) 7_575 6_565 ?
V Ca V 109.8(2) 5_565 6_565 ?
08 Ca Si1 118.8(6) . 7_575 ?
02 Ca Si1 126.5(3) 4_464 7_575 ?
02 Ca Si1 69.4(3) 6_565 7_575 ?
01 Ca Si1 22.31(14) 7_575 7_575 ?
01 Ca Si1 95.2(5) . 7_575 ?
07 Ca Si1 98.0(14) . 7_575 ?
07 Ca Si1 115.6(13) 7_575 7_575 ?
07B Ca Si1 85.6(14) . 7_575 ?
07B Ca Si1 102.6(14) 7_575 7_575 ?
V Ca Si1 58.7(2) 5_565 7_575 ?
V Ca Si1 101.42(15) 6_565 7_575 ?
01 Si1 O3 111.6(4) . . ?
01 Si1 O5 109.8(3) . . ?
03 Si1 O5 106.5(4) . . ?
01 Si1 O4 111.7(3) . . ?
03 Si1 O4 107.9(4) . . ?
05 Si1 O4 109.2(5) . . ?
01 Si1 Ca 32.9(3) . . ?
03 Si1 Ca 109.9(3) . . ?
05 Si1 Ca 79.6(4) . . ?
04 Si1 Ca 136.6(2) . . ?
02 Si2 O3 110.9(3) . . ?
02 Si2 O4 109.0(4) . 5_565 ?
03 Si2 O4 109.1(4) . 5_565 ?
02 Si2 O5 109.3(4) . 4_465 ?
03 Si2 O5 107.5(5) . 4_465 ?
04 Si2 O5 111.0(4) 5_565 4_465 ?
02 Si2 Ca 30.7(3) . 6_556 ?
03 Si2 Ca 118.3(3) . 6_556 ?
04 Si2 Ca 125.9(3) 5_565 6_556 ?
05 Si2 Ca 78.9(4) 4_465 6_556 ?
Si1 O1 V 133.7(4) . 5_565 ?
Si1 O1 Ca 124.8(4) . . ?
V O1 Ca 100.3(5) 5_565 . ?
Si2 O2 V 125.4(4) . . ?
Si2 O2 Ca 128.4(3) . 6_556 ?
V O2 Ca 105.7(5) . 6_556 ?
Si1 O3 Si2 137.3(4) . . ?
Si1 O4 Si2 127.0(5) . 5_565 ?
Si1 O5 Si2 126.2(4) . 4_464 ?
07 O7 O7B 91(5) 7_575 . ?
07 O7 O7B 52(3) 7_575 7_575 ?
07B O7 O7B 39(6) . 7_575 ?
07 O7 O8 73(2) 7_575 . ?
07B O7 O8 144(7) . . ?
07B O7 O8 117(5) 7_575 . ?
07 O7 Ca 80.1(13) 7_575 . ?
07B O7 Ca 83(4) . . ?
07B O7 Ca 78(4) 7_575 . ?
08 O7 Ca 63(4) . . ?

07B 07B 07 89(5) 7_575 . ?
07B 07B 07 52(3) 7_575 7_575 ?
07 07B 07 37(5) . 7_575 ?
07B 07B Ca 80.1(14) 7_575 . ?
07 07B Ca 71(4) . . ?
07 07B Ca 69(3) 7_575 . ?
07 08 07 34(5) 7_575 . ?
07 08 Ca 82(5) 7_575 . ?
07 08 Ca 82(5) . . ?

_diffrn_measured_fraction_theta_max 0.976
_diffrn_reflns_theta_full 23.85
_diffrn_measured_fraction_theta_full 0.976
_refine_diff_density_max 0.790
_refine_diff_density_min -0.779
_refine_diff_density_rms 0.155